26. Stankiewicz, P., Shaw, C.J., Withers, M., Inoue, K. and Lupski, J.R. (2004) Serial segmental duplications during primate evolution result in complex human genome architecture. *Genome Res.*, **14**, 2209–2220.
27. Kurotaki, N., Stankiewicz, P., Wakui, K., Niikawa, N. and Lupski, J.R. (2005) Sotos syndrome common deletion is mediated by directly oriented subunits within inverted Sos-REP low-copy repeats. *Hum. Mol. Genet.*, **14**, 535–542.
28. Visser, R., Shimokawa, O., Harada, N., Kinoshita, A., Ohta, T., Niikawa, N. and Matsumoto, N. (2005) Identification of a 3.0-kb major recombination hotspot in patients with Sotos syndrome who carry a common 1.9-Mb microdeletion. *Am. J. Hum. Genet.*, **76**, 52–67.
29. Lee, J.A., Madrid, R.E., Sperle, K., Ritterson, C.M., Hobson, G.M., Garbern, J., Lupski, J.R. and Inoue, K. (2006) Spastic paraplegia type 2 associated with axonal neuropathy and apparent *PLP1* position effect. *Ann. Neurol.*, **59**, 398–403.
30. Hodes, M.E., Woodward, K., Spinner, N.B., Emanuel, B.S., Enrico-Simon, A., Kamholz, J., Stambolian, D., Zackai, E.H., Pratt, V.M., Thomas, I.T. *et al.* (2000) Additional copies of the proteolipid protein gene causing Pelizaeus-Merzbacher disease arise by separate integration into the X chromosome. *Am. J. Hum. Genet.*, **67**, 14–22.
31. Iwaki, A., Kondo, J., Ototsuji, M., Kurosawa, K. and Fukumaki, Y. (2003) Characterization of the breakpoints of PLP1 duplication in three cases of Pelizaeus-Merzbacher disease. *Am. J. Hum. Genet.*, **73** (suppl.), 549.
32. Shaw, C.J. and Lupski, J.R. (2005) Non-recurrent 17p11.2 deletions are generated by homologous and non-homologous mechanisms. *Hum. Genet.*, **116**, 1–7.
33. Mimault, C., Giraud, G., Courtois, V., Cailloux, F., Boire, J.Y., Dastugue, B. and Boespflug-Tanguy, O. (1999) Proteolipoprotein gene analysis in 82 patients with sporadic Pelizaeus-Merzbacher Disease: duplications, the major cause of the disease, originate more frequently in male germ cells, but point mutations do not. The Clinical European Network on Brain Dysmyelinating Disease. *Am. J. Hum. Genet.*, **65**, 360–369.
34. Hu, X., Ray, P.N. and Worton, R.G. (1991) Mechanisms of tandem duplication in the Duchenne muscular dystrophy gene include both homologous and nonhomologous intrachromosomal recombination. *EMBO J.*, **10**, 2471–2477.
35. Heath, J.D. and Weinstock, G.M. (1991) Tandem duplications of the *lac* region of the *Escherichia coli* chromosome. *Biochimie*, **73**, 343–352.
36. Woodward, K., Cundall, M., Palmer, R., Surtees, R., Winter, R.M. and Malcolm, S. (2003) Complex chromosomal rearrangement and associated counseling issues in a family with Pelizaeus-Merzbacher disease. *Am. J. Med. Genet.*, **118A**, 15–24.
37. Ida, T., Miharu, N., Hayashitani, M., Shimokawa, O., Harada, N., Samura, O., Kubota, T., Niikawa, N. and Matsumoto, N. (2003) Functional disomy for Xq22-q23 in a girl with complex rearrangements of chromosomes 3 and X. *Am. J. Med. Genet.*, **120A**, 557–561.
38. Wolf, N.I., Sistermans, E.A., Cundall, M., Hobson, G.M., Davis-Williams, A.P., Palmer, R., Stubbs, P., Davies, S., Endziniene, M., Wu, Y. *et al.* (2005) Three or more copies of the proteolipid protein gene *PLP1* cause severe Pelizaeus-Merzbacher disease. *Brain*, **128**, 743–751.
39. Combes, P., Bonnet-Dupeyron, M.-N., Gauthier-Barichard, F., Schiffmann, R., Bertini, E., Rodriguez, D., Armour, J.A.L., Boespflug-Tanguy, O. and Vaurs-Barrière, C. (2006) *PLP1* and *GPM6B* intragenic copy number analysis by MAPH in 262 patients with hypomyelinating leukodystrophies: identification of one partial triplication and two partial deletions of. *PLP1. Neurogenetics*, **7**, 31–37.
40. Eichler, E.E. (1998) Masquerading repeats: paralogous pitfalls of the human genome. *Genome Res.*, **8**, 758–762.
41. Johnson, R.D. and Jasin, M. (2000) Sister chromatid gene conversion is a prominent double-strand break repair pathway in mammalian cells. *EMBO J.*, **19**, 3398–3407.
42. Richardson, C. and Jasin, M. (2000) Coupled homologous and nonhomologous repair of a double-strand break preserves genomic integrity in mammalian cells. *Mol. Cell. Biol.*, **20**, 9068–9075.
43. Tatusova, T.A. and Madden, T.L. (1999) BLAST 2 sequences, a new tool for comparing protein and nucleotide sequences. *FEMS Microbiol. Lett.*, **174**, 247–250.
44. Kent, W.J., Sugnet, C.W., Furey, T.S., Roskin, K.M., Pringle, T.H., Zahler, A.M. and Haussler, D. (2002) The human genome browser at UCSC. *Genome Res.*, **12**, 996–1006.
45. Karolchik, D., Baertsch, R., Diekhans, M., Furey, T.S., Hinrichs, A., Lu, Y.T., Roskin, K.M., Schwartz, M., Sugnet, C.W., Thomas, D.J. *et al.* (2003) The UCSC Genome Browser Database. *Nucleic Acids Res.*, **31**, 51–54.
46. Inoue, K., Kanai, M., Tanabe, Y., Kubota, T., Kashork, C.D., Wakui, K., Fukushima, Y., Lupski, J.R. and Shaffer, L.G. (2001) Prenatal interphase FISH diagnosis of *PLP1* duplication associated with Pelizaeus-Merzbacher disease. *Prenat. Diagn.*, **21**, 1133–1136.
47. Lee, J.A., Cheung, S.W., Ward, P.A., Inoue, K. and Lupski, J.R. (2005) Prenatal diagnosis of *PLP1* copy number by array comparative genomic hybridization. *Prenat. Diagn.*, **25**, 1188–1191.
48. Potocki, L., Chen, K.-S., Park, S.-S., Osterholm, D.E., Withers, M.A., Kimonis, V., Summers, A.M., Meschino, W.S., Anyane-Yeboa, K., Kashork, C.D. *et al.* (2000) Molecular mechanism for duplication 17p11.2—the homologous recombination reciprocal of the Smith-Magenis microdeletion. *Nat. Genet.*, **24**, 84–87.

Available online at www.sciencedirect.com
ScienceDirect
Biochemical and Biophysical Research Communications 350 (2006) 82–90
BBRC
www.elsevier.com/locate/ybbrc

Monoubiquitylation of GGA3 by hVPS18 regulates its ubiquitin-binding ability

Satomi Yogosawa [a,b], Masato Kawasaki [c], Soichi Wakatsuki [c], Eiki Kominami [d], Yoko Shiba [e], Kazuhisa Nakayama [e], Shinichi Kohsaka [a,*], Chihiro Akazawa [a]

[a] *Department of Neurochemistry, National Institute of Neuroscience, NCNP, Kodaira, Tokyo 187-8502, Japan*
[b] *Division of Molecular Biology, Research Institute for Biological Sciences, Tokyo University of Science, Noda, Chiba 278-0022, Japan*
[c] *Structural Biology Research Center, Photon Factory, Institute of Materials Structure Science, High Energy Accelerator Research Organization (KEK), Tsukuba, Ibaraki 305-0801, Japan*
[d] *Department of Biochemistry, Juntendo University School of Medicine, Bunkyo-ku, Tokyo 113-8421, Japan*
[e] *Graduate School of Pharmaceutical Science, Kyoto University, Sakyo-ku, Kyoto 606-8501, Japan*

Received 25 August 2006
Available online 15 September 2006

Abstract

GGAs (Golgi-localizing, γ-adaptin ear domain homology, ADP-ribosylation factor (ARF)-binding proteins), constitute a family of monomeric adaptor proteins and are associated with protein trafficking from the *trans*-Golgi network to endosomes. Here, we show that GGA3 is monoubiquitylated by a RING-H2 type-ubiquitin ligase hVPS18 (human homologue of *vacuolar protein sorting* 18). By *in vitro* ubiquitylation assays, we have identified lysine 258 in the GAT domain as a major ubiquitylation site that resides adjacent to the ubiquitin-binding site. The ubiquitylation is abolished by a mutation in either the GAT domain or ubiquitin that disrupts the GAT-ubiquitin interaction, indicating that the ubiquitin binding is a prerequisite for the ubiquitylation. Furthermore, the GAT domain ubiquitylated by hVPS18 no longer binds to ubiquitin, indicating that ubiquitylation negatively regulates the ubiquitin-binding ability of the GAT domain. These results suggest that the ubiquitin binding and ubiquitylation of GGA3-GAT domain are mutually inseparable through a ubiquitin ligase activity of hVPS18.

Keywords: GGA; GAT-domain; hVPS18; RING-H2 domain; Ubiquitin ligase; Monoubiquitylation; Ubiquitin-binding

In eukaryotic cells, vesicular trafficking of proteins between intracellular compartments, such as the Golgi complex and the multivesicular body (MVB)/lysosome, plays an important role in cellular functions. GGAs (Golgi-localizing, γ-adaptin ear domain homology, ADP-ribosylation factor (ARF)-binding proteins) are a family of monomeric adaptor proteins that regulate delivery of clathrin-coated vesicles from the TGN to endosomes [1–3]. In mammals, there are three GGAs (GGA1, GGA2, and GGA3) that share four functional domains, named VHS (Vps27/Hrs/Stam), GAT (GGA and Tom1 (target of Myb 1)), hinge, and GAE (γ-adaptin ear) [4–7]. The N-terminal VHS domain directly binds to acidic cluster-dileucine motifs found in the cytoplasmic domains of transmembrane cargo proteins [8–10]. The GAT domain is responsible for association of GGAs with the TGN membrane through interacting with activated ARF (a GTP-bound form) [11]. The proline-rich hinge region, the most variable among the GGA isoforms, mediates recruitment of clathrin [12]. The C-terminal GAE domain associates with various accessory proteins that modulate vesicle transport [1,3].

In the past few years, a number of proteins that are involved in membrane trafficking, especially in endocytosis and degradation in lysosomes, have been shown to be

* Corresponding author. Fax: +81 42 346 1751.
E-mail address: kohsaka@ncnp.go.jp (S. Kohsaka).

0006-291X/$ - see front matter © 2006 Elsevier Inc. All rights reserved.
doi:10.1016/j.bbrc.2006.09.013

functionally modulated by their ubiquitin binding and ubiquitylation [13–16]. Recently, it has also been shown that ubiquitin binding and ubiquitylation play an important role in selective transport of proteins from the TGN. The GAT domains of GGAs bind to ubiquitin and/or ubiquitylated proteins and undergo monoubiquitylation in the cell [17–20]. The interaction between the GAT domain and ubiquitin may endow GGAs with the ability to sort ubiquitylated transmembrane proteins at both the TGN and endosomes. Several ubiquitin ligases (E3) have been shown to be involved in monoubiquitylation of membrane-associated proteins and to participate in the endocytic and degradation pathways [21]. For example, c-Cbl, a RING-type ligase, ubiquitylates epidermal growth factor receptor (EGFR) depending on ligand-stimulated phosphorylation of the receptor [22], and Nedd4, a HECT-type ligase, is required for monoubiquitylation of eps15 and Hrs [23,24].

The Class C Vps (vacuolar protein sorting) complex is required for vesicle transport from the late endosome to vacuole in yeast [25,26]. In mammals, VPS proteins also appear to control the fusion events of late endosomes and lysosomes [27,28]. In humans, four Class C VPS proteins, hVPS11, hVPS16, hVPS18, and hVPS33, constitute a large hetero-oligomeric complex that interacts with syntaxin 7 at late endosomes/lysosomes [29]. Moreover, they also exist as a large detergent-insoluble HOPS (homotypic fusion and vacuole protein sorting) complex that contains additional components, hVPS39/Vam6, and hVPS41/Vam2 [27]. Overexpression of VPS39/Vam6S alters the late endosome function in mammalian cells [30]. Thus, it is necessary to discuss specific functions of Class C VPS proteins based on the biochemical properties.

In this report, we have demonstrated that GGAs (GGA1 and GGA3 but not GGA2) are monoubiquitylated by hVPS18, a RING-H2 type ubiquitin ligase, and identified a lysine residue in the C-terminal subdomain of the GAT domain as a major ubiquitylation site. Furthermore, we have shown that the monoubiquitylation negatively regulates the ubiquitin-binding ability of GGA itself. These observations shed light on the regulatory mechanisms of GGA to participate in membrane trafficking through the association of hVPS18.

Materials and methods

Plasmid construction. Full-length and various truncated human GGA cDNAs, as described previous, [17], were subcloned into the following vector: the pGEX-4T2 (Amersham Biosciences) prokaryotic expression vector for the production of GST-tagged fusion proteins. Myc-tagged hVPS18 and hVPS11 mammalian expression vectors were prepared as described previously [29]. The full-length hVPS18, hVPS11, and hVPS16 were subcloned into pFastBacHTb insect expression vector (Invitrogen) to generate His_6-tagged fusion proteins.

Expression and preparation of recombinant proteins. E2 ubiquitin-conjugating enzyme, human Ubc4, was produced in *Escherichia coli* strain BL21-AI (Invitrogen). GST-GGA (wild-type and truncated mutants) and GST-ubiquitin (Ub) (wild-type and mutants) were expressed in *E. coli* strain BL21-AI and the recombinant proteins were purified by using glutathione–Sepharose 4B beads (Amersham Biosciences) in PBS containing 1 mM PMSF, Complete protease inhibitor mixture, and 1% Triton X-100. His_6-tagged hVPS18, hVPS11, and hVPS16 were expressed in Sf-9 insect cells using baculovirus protein expression system (Invitrogen) and the recombinant proteins were purified under the denatured condition (8 M urea), and followed by using TALON metal affinity beads (BD Biosciences), and renatured in PBS. Circular dichroism spectra of the wild-type and mutant proteins were recorded on a Jasco J-820 spectropolarimeter at 25 °C using a cuvette with 1 mm path length with the protein concentration of 30 μM in PBS.

Antibody. Polyclonal antibody against human GGA1, GGA2, and GGA3 was raised in rats by immunization with purified full-length GGA1, GGA2, and GGA3, respectively. These antibodies were affinity-purified on HiTrap NHS-activated columns (Amersham Biosciences) conjugated with immunogens. Monoclonal GGA3 antibody was purchased from BD Transduction Laboratories. Anti-hVPS18, hVPS11, and hVPS16 antibodies were prepared as described previously [29].

Immunocytochemistry. HeLa cells were immunostained with mouse anti-GGA3 antibody and rabbit anti-hVPS18 as described previously [29]. To confirm intracellular colocalization, immunoreactivities were analyzed by the sectioning microscope (Delta Vision) calibrated by using fluorescent beads (TetraSpeck Fluorescent Microsphere Standards, 0.1 μm, Invitrogen).

Immunoprecipitation. Immunoprecipitation was performed as described previously [29]. Briefly, the cells were transfected with various plasmids by Fugene 6 reagent (Roche Molecular Biochemicals) according to the manufacturer's instructions. At 24 h after transfection, total cell lysates were incubated with 4 μg of anti-FLAG antibodies (monoclonal M2, Sigma) at 4 °C overnight. Immunoprecipitation of the antigen-antibody complex was accomplished by adding 40 μl of protein G–Sepharose for 1 h at 4 °C. Sepharose bound proteins were subjected to SDS–PAGE and detected by Western blot analyses with anti-Myc antibody (Roche Molecular Biochemicals) or anti-FLAG M2 antibody, respectively.

In vitro pull-down assay. In vitro pull-down assay was performed as described previously [31]. Briefly, GST-GGA-GAT proteins were immobilized on glutathione–Sepharose 4B beads and incubated with His_6-hVPS18 at 25 °C for 30 min. The resin was washed, subjected to SDS–PAGE, and detected by Western blot analyses with either anti-His_6 antibody (Santa Cruz Biotechnology) or anti-GST antibody.

We performed assays of GGA3 binding to ubiquitin as described previous [17]. Briefly, various GGA3 proteins were incubated with Ub-(10 μl) or protein A–agarose (15 μl) beads (Sigma) for 1 h at room temperature. The beads were washed, subjected to SDS–PAGE, and detected by Western blot analyses using anti-GST antibody.

To prepare ubiquitylated GGA3 C-GAT proteins, GGA3 C-GAT proteins were subjected to *in vitro* ubiquitylation assay and immobilized on glutathione–Sepharose 4B beads. The beads were then washed with a buffer (25 mM Hepes, pH 7.4, 0.1% Nonidet P-40, 0.5 M NaCl, and 50% ethylene glycol) and eluted with 25 mM Hepes, pH 7.4, 20 mM reduced glutathione.

In vitro ubiquitylation assay. An *in vitro* ubiquitylation assay was performed as described previously [29]. Briefly, GST-GGA proteins were mixed with yeast E1 (500 ng) (Boston Biochem), human Ubc4, ubiquitin (Boston Biochem) or GST-Ub (10 or 5 μg, respectively), and His_6-tagged hVPS18 (or hVPS11 or hVPS16). The mixture was incubated at 25 °C for 30 or 60 min in the presence of 50 mM Tris–HCl, pH 7.4, 5 mM $MgCl_2$, 2 mM dithiothreitol (DTT), and 4 mM ATP in a 20 μl volume. After incubation, the mixtures were immobilized on glutathione–Sepharose 4B beads and washed with wash buffer for three times. The resin was subjected to SDS–PAGE and detected by Western blot analyses using anti-GST antibody or anti-His_6 antibody or specific antibody.

Results and discussion

Direct interaction with GGAs and hVPS18

Recent studies identified the GAT domain as a ubiquitin-binding module [17–20]. Furthermore, our recent yeast

two-hybrid screening using hVPS18 as bait identified a partial fragment of GGA3 [31]. We first confirmed the molecular interaction by an *in vitro* pull-down assay using recombinant GGAs and hVPS18. As shown in Fig. 1A, His_6-hVPS18 was pulled down with the GST fusion of the GAT domain of GGA1, GGA2 or GGA3. We next analyzed the *in vivo* interaction by a co-immunoprecipitation experiment using lysates of cells cotransfected with FLAG-GGAs and either Myc-hVPS18 or Myc-hVPS11. As shown in Fig. 1B, all GGAs co-immunoprecipitated hVPS18. By contrast, either GGA could not interact with hVPS11, another Class C component having a RING-H2

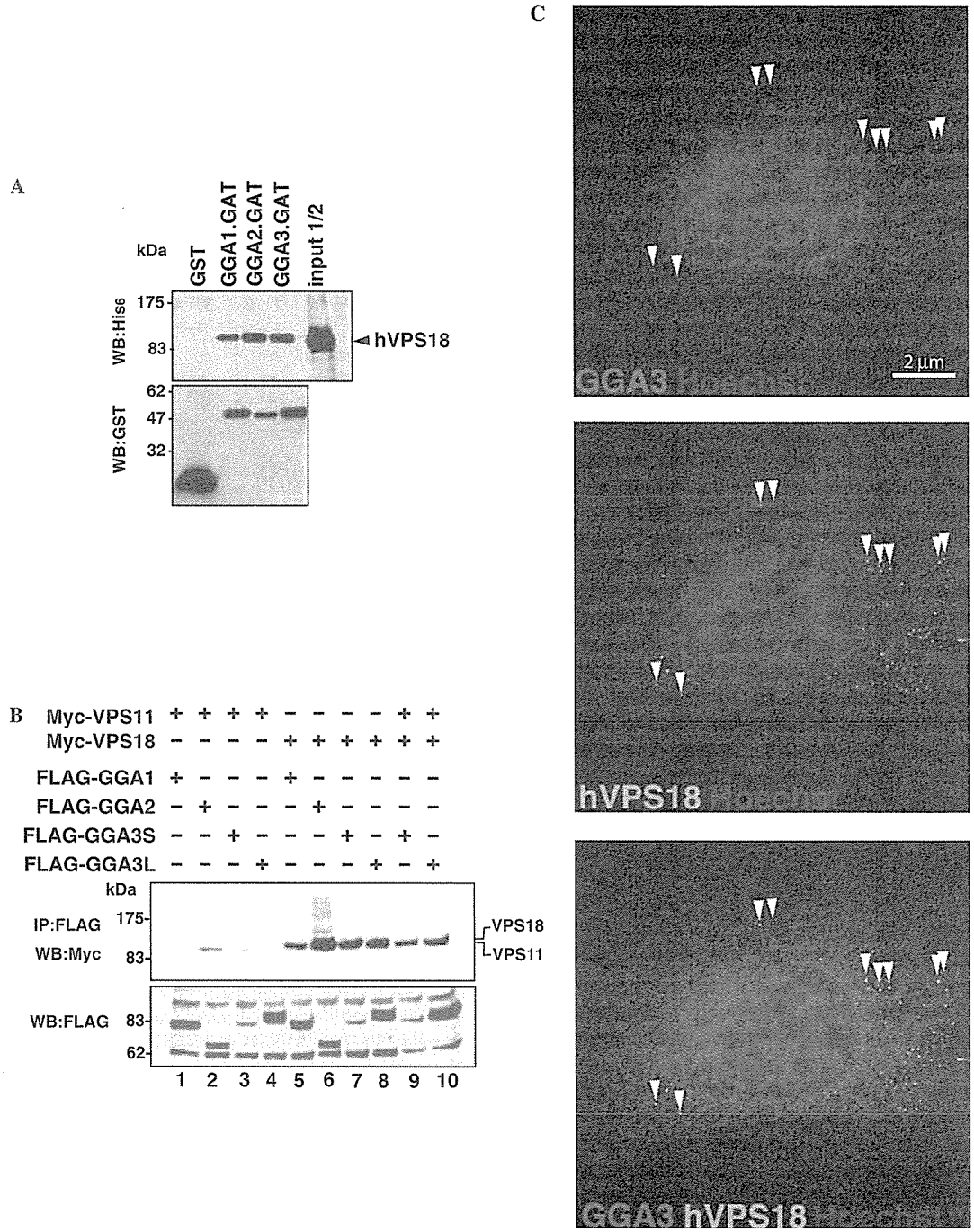

Fig. 1. GGA-GAT domains interact with hVPS18. (A) His_6-hVPS18 bound to three GST-GGA-GAT proteins was detected by Western blot analyses using anti-GST antibody. (B) Cos7 cells were co-transfected with His_6-FLAG-GGAs and Myc-hVPS11 or hVPS18. At 24 h post-transfection, whole-cell lysates were co-immunoprecipitated using anti-FLAG M2 antibody. Immunoprecipitates were resolved by SDS–PAGE and detected by Western blot analyses using indicated antibody. (C) The interaction of endogenous GGA3 (*Red*) and hVPS18 (*Green*) in HeLa cells was detected by immunocytochemistry. Colocalizing profiles are pointed out with *arrows*. *Bar*, 2 μm.

domain. Considering the molecular interaction between GGAs and hVPS18, a major issue that arises is the intracellular localization of these proteins. GGAs have been characterized as TGN-associated clathrin adaptors, whereas the Class C VPS complex has been proposed to function in endosomal/lysosomal compartments. We therefore analyzed the precise intracellular localization of endogenous GGA3 and hVPS18 in HeLa cells by the sectioning microscopy. The optical pathways were calibrated using fluorescent labeled beads (0.1 μm diameter). The thirty series of sections covering 5 μm thickness were captured and deconvoluted images were analyzed. As shown in a representative image Fig. 1C, GGA3 immunoreactivities (colored in *Red*) and hVPS18 immunoreactivities (colored in *Green*) were often colocalized on punctuates (colored in *Yellows*) of perinuclear structures (indicated by arrowheads).

Monoubiquitylation of GGAs by hVPS18, RING-H2 type ubiquitin ligase

Our recent study, showed that the RING-H2 domain of hVPS18 displays a E3 ubiquitin ligase activity [31]. To examine whether GGAs are ubiquitylated by the hVPS18, we performed an *in vitro* ubiquitylation assay using full-length GGAs as substrates. As shown in Fig. 2A, the molecular weight of GGA1 and GGA3 was shifted by ~8 kDa only in the simultaneous presence of ubiquitin, E1, E2 (UbcH4), and hVPS18 (lanes 2 and 6, respectively). By contrast, the shift was not observed in the case of GGA2 (lane 4), being compatible with our previous study showing that GGA2 is not able to interact with ubiquitin nor ubiquitylated in the cell. We next examined whether the *in vitro* modification represents monoubiquitylation/multiubiquitylation or not. In this experiment, we used wild-type (WT) ubiquitin fused to GST, and its K48R and KO (all lysine residues were replaced with arginine) mutants, since these mutants are not conjugated to conventional polyubiquitin chains. As shown in Fig. 2B, when GST-ubiquitin WT was used, the molecular weight of the GGA3-GAT domain was shifted by 35 kDa, which corresponds to the size of GST-ubiquitin. Essentially the same band shift was observed using the K48R and KO mutants, indicating that GGA3 is mainly monoubiquitylated by hVPS18.

Since hVPS18 forms a complex with other Class C VPS components [29], we then examined whether hVPS11 and hVPS16 were also involved in the monoubiquitylation of GGA3. Although hVPS11 also has a RING-H2 domain and shows a ubiquitin ligase activity (data not shown), it did not ubiquitylate the GGA3-VHS+GAT domain irrespective of the presence of hVPS16 (Fig. 2C lanes 2 and 3). However, the monoubiquitylation of GGA3 by hVPS18 was extremely enhanced in the presence of hVPS11 and hVPS16 (compare lane 5 with lanes 6 and 7). This result makes it likely that hVPS18 is involved in the monoubiquitylation of GGA3 as a Class C VPS complex.

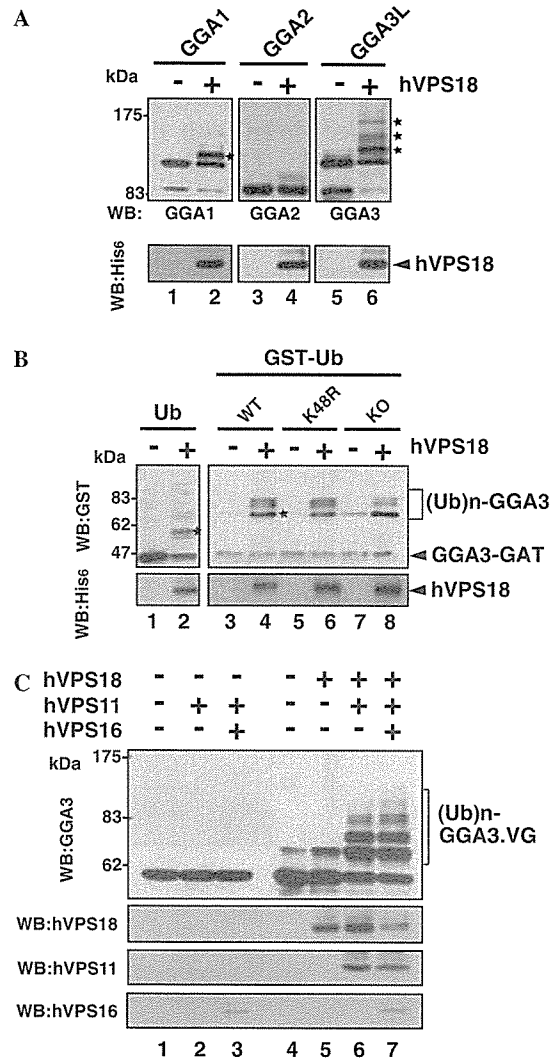

Fig. 2. GGAs are monoubiquitylated by hVPS18. (A) The *in vitro* ubiquitylation of GST-GGAs wild-type by His_6-hVPS18. The sample was detected by Western blot analyses using anti-GGA1, GGA2, or GGA3 (upper panel). Purified His_6-hVPS18 protein was detected by Western blot analyses using anti-His_6 antibody (lower panel). Asterisks represent ubiquitylated form of GGAs. (B) The *in vitro* ubiquitylation of GST-GGA3-GAT protein in the presence of no-tagged ubiquitin (Ub) or GST-fused ubiquitin (GST-Ub); wild-type (WT), K48R, or all lysines mutated to arginines (KO). The sample was detected by Western blot analyses using anti-GST or anti-His_6 antibody. Asterisks represent ubiquitylated forms of GGA3 that conjugate to Ub (left panel) or GST-Ub (right panel). (C) The *in vitro* ubiquitylation of GST-GGA3-VG (VHS+GAT) by hVPS11 or hVPS18 in the presence or absence of hVPS16. Purified His_6-tagged hVPS18 (or hVPS11 or hVPS16) protein was detected by Western blot analyses using specific antibodies.

Ubiquitin binding-dependent monoubiquitylation of GGA3-GAT

Identification of the ubiquitylation site is of great significance to discuss the molecular mechanism underlying the GGA ubiquitylation. We have recently shown that GGA3 is ubiquitylated in the C-terminal subdomain of its GAT domain (C-GAT) *in vivo* [17]. We therefore,

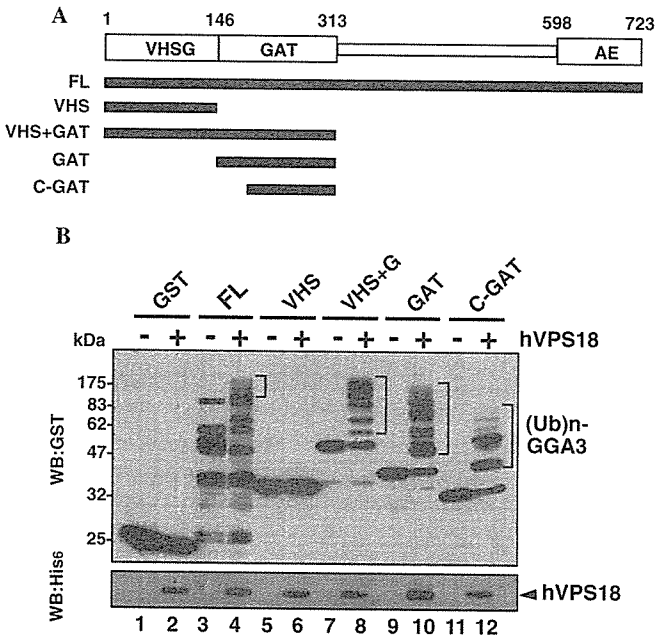

Fig. 3. GGA3 is ubiquitylated in the C-GAT domain. (A) Schematic representation of GGA3. (B) The *in vitro* ubiquitylation of GST-GGA3 full-length or truncated mutants. The sample was detected by Western blot analyses using anti-GST or anti-His_6 antibody. The positions of ubiquitylated GGA3 are indicated by a bracket.

performed an *in vitro* ubiquitylation assay using various truncation mutants of GGA3 (Fig. 3A). As shown in Fig. 3B, ubiquitylation occurred in the GGA3 fragments covering the C-GAT subdomain (lanes 4, 8, 10, and 12) but not in the GST protein (lane 2) nor the VHS domain alone (lane 6), in agreement with our previous ubiquitylation data in the cell [17].

Recent studies have shown, that many proteins containing ubiquitin-binding modules undergo monoubiquitylation and more importantly, their ubiquitin-binding ability is required for their own monoubuquitylation [23,32,33]. Therefore, we tested *in vitro* whether various GGA3 mutants that lack ubiquitin-binding ability were monoubiquitylated by hVPS18. As shown in Supplementary Fig. 1, the GGA3-GAT helix α3 mutant (L280R or D284G) defective in ubiquitin binding was not monoubiquitylated (compare lane 2 with lanes 6 and 8). Essentially the same result was obtained with a GGA3-GAT helix α2/α3 double mutant, E250N/D284G. These results indicate that binding to ubiquitin is a prerequisite for the GGA3 ubiquitylation. Next we constructed various truncated mutants of the GGA3-GAT domain (Supplementary Fig. 2A) and compared their ubiquitin binding (in Supplementary Fig. 2B) and ubiquitylation by hVPS18 (Supplementary Fig. 2C). Remarkably, all of the GAT fragments that retained ubiquitin-binding ability were monoubiquitylated by hVPS18, whereas the fragments lacking the ability were not monoubiquitylated. These data indicate that binding to ubiquitin and ubiquitylation of the GAT domain are intimately coupled events.

Lys258 is the major ubiquitylation site

In the C-GAT subdomain of GGA3, there are six lysine residues that can be conjugated to ubiquitin. To determine which lysine residue(s) was ubiquitylated, we systematically replaced the lysine residues with arginines (Fig. 4A) and examined binding to ubiquitin and monoubiquitylation of these lysine mutants. As shown in Fig. 4B, all of the C-GAT mutants examined retained their ubiquitin-binding ability. In striking contrast, they were variable in the ubiquitylation efficiency (Fig. 4C). Namely, (i) a mutant, 5KR(258), in which all the lysine residues except for K258 were replaced with arginines (Fig. 4A), underwent monoubiquitylation (lane 10) at comparable efficiency to that of the WT C-GAT subdomain (lane 2); (ii) the 5KR(249), 5KR(264), and 5KR(294) mutants underwent ubiquitylation at extremely low efficiency (lanes 8, 12, and 14); and (iii) ubiquitylation of 5KR(210), 5KR(213), and 6KR mutants was under the detection level (lanes 4, 6, and 16). As shown in Supplemental Figure 4, the circular dichroism spectra of WT and 5KR(258) were almost identical, suggesting that the mutations did not significantly affect the overall conformation of the C-GAT subdomain. Taken together, we conclude that lysine 258 is the major site ubiquitylated by hVPS18, although other lysine residues at positions 249, 264, and 294 were also ubiquitylated to some extent.

Model of GGA3-GAT domain ubiquitylated at Lys258

Previously, we determined the crystal structure of the complex between GGA3 C-GAT and ubiquitin, and showed primarily hydrophobic interactions in which the site 1 in C-CAT constitutes the binding site with three times higher affinity than the site 2 [34]. To understand the molecular basis for the coupling of ubiquitin binding and ubiquitylation of the GGA3-GAT domain, we mapped the positions of lysine residues of GGA3 C-GAT in the complex structure (Fig. 5). Among the six candidate lysine residues, lysine 258 is the closest to the C-terminus of ubiquitin (Fig. 5, Table 1), suggesting that this lysine is most susceptible to ubiquitin conjugation. This model also suggests that no major structural rearrangement between ubiquitin and the GGA3 C-GAT domain is required for the ubiquitylation of lysine 258.

Ubiquitylated GGA3 C-GAT loses its ubiquitin-binding ability

Hicke et al. have proposed a possibility that ubiquitylation of ubiquitin-binding proteins might generally have a regulatory function by affecting association of their ubiquitin-binding modules with either free ubiquitin or ubiquitylated proteins [13]. To address this possibility, we performed *in vitro* pull-down assay using reaction products of the *in vitro* ubiquitylation, in which both ubiquitylated and non-ubiquitylated C-GAT proteins were included. As

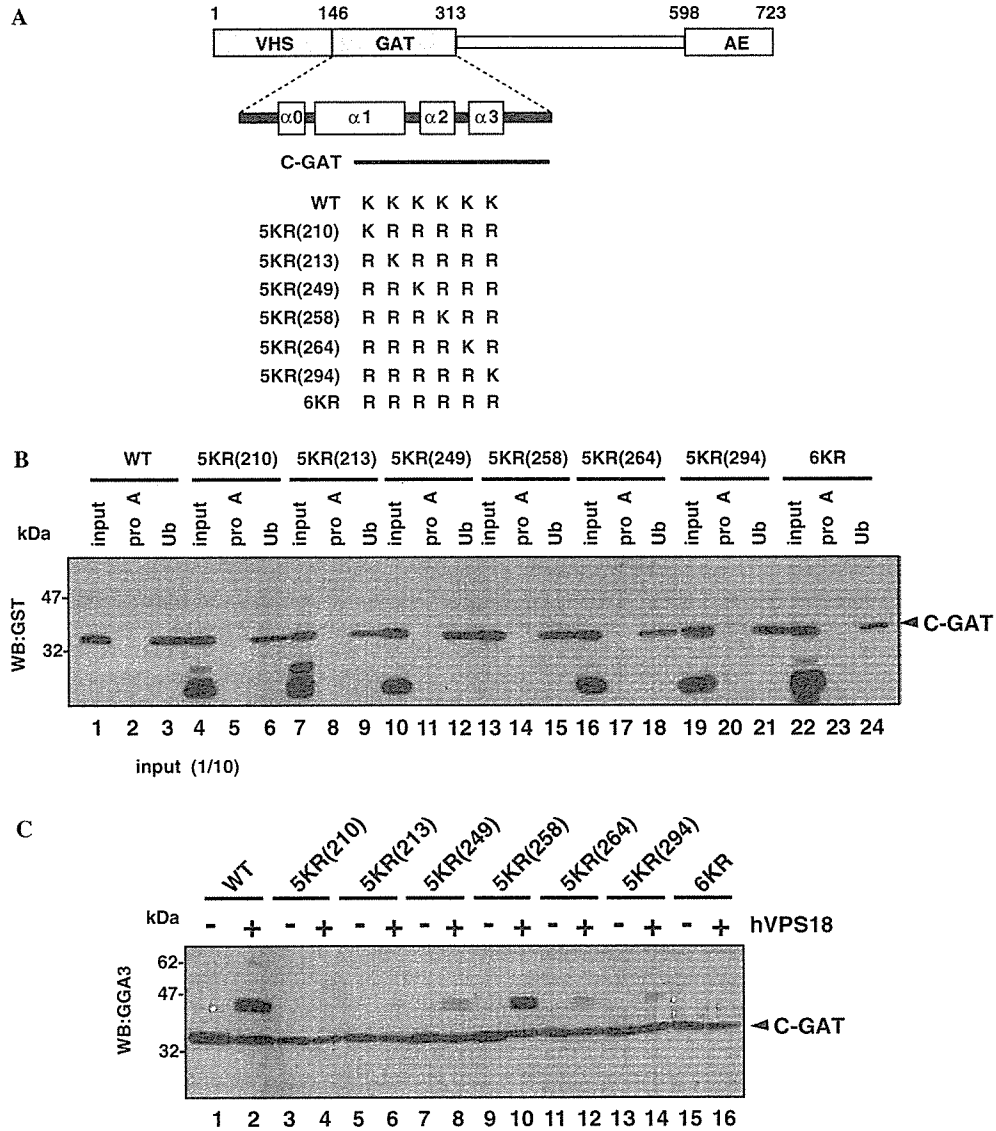

Fig. 4. GGA3 is mainly ubiquitylated at lysine 258 that resides in the two ubiquitin-binding sites. (A) Schematic representation of GGA3-GAT. (B) The *in vitro* pull-down assay of GGA3 C-GAT. Equal amounts of purified GGA3 C-GAT proteins were incubated with Ub- or Protein-A–agarose. The resin was washed, subjected to SDS–PAGE, and detected by Western blot analyses with anti-GST antibody. Ten percent of input samples were loaded on *input lanes*. (C) The *in vitro* ubiquitylation of GST-GGA3 C-GAT proteins. The sample was detected by Western blot analyses using anti-GGA3 antibody.

shown in Fig. 6, the ubiquitylated form of C-GAT WT or its 5KR(258) mutant was not pulled down with ubiquitin-agarose beads (lanes 3 and 7, indicated by asterisks), whereas their non-ubiquitylated forms were pulled down well. This result indicates that covalent modification by ubiquitin at lysine 258 makes C-GAT inaccessible to ubiquitin.

Recent advances have uncovered that several membrane-trafficking events are mediated by ubiquitin binding and monoubiquitylation, including changes in subcellular localization, protein conformation, activity, and protein-protein interaction. [16,35,36]. GGA might have evolved to allow a wide variety of proteins to interact directly with ubiquitin or ubiquitylated proteins during various cellular processes [1,20,37,38]. In this study, we first identified that hVPS18 acts as a genuine ubiquitin ligase of GGAs (Fig. 2A). The modification by hVPS18 slightly differs among GGAs; the monoubiquitylation occurs in one or multiple lysine sites of GGA1 and GGA3 but not of GGA2 (Figs. 2A and B). We then focused on GGA3 and tried to identify the responsible lysine. By taking an advantage of E3 identification, we utilized various KR mutants (Fig. 4). Finally, we identified the lysine 258 is the main target lysine for the ubiquitylation by hVPS18. If we closely look at the results of co-crystallization of GGA3 C-GAT and ubiquitin, the lysine 258 is located at the closest position to the C-terminus of ubiquitin, suggesting that the ubiquitin binding is necessary for ubiquitylation.

It has been recently shown that a free ubiquitin or ubiquitylated proteins are recognized by small (20–150 amino

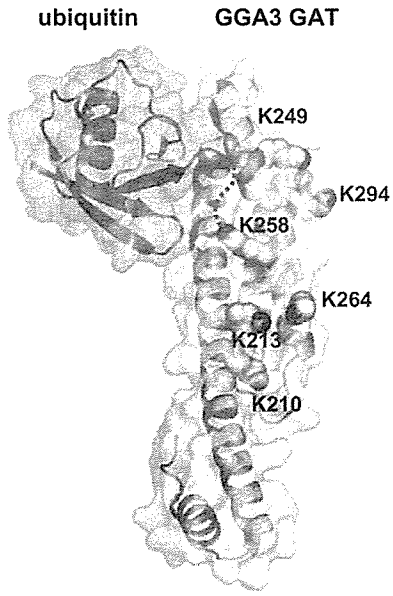

Fig. 5. Molecular surface representation of GGA3 C-GAT. The model was built by combining the crystal structures of the complex between ubiquitin and GGA3 C-GAT subdomain [34] and the entire GGA1 GAT domain [44]. Ubiquitin and GGA3 GAT domain are shown as ribbon diagrams with transparent surface representations (ubiquitin, *Orange*; GGA3 GAT, *Green*). Six lysine residues of the GGA3 C-GAT subdomain are shown with space-filling atoms (carbon atoms, *Yellow*; nitrogen atoms, blue). The C-terminal of ubiquitin (The last visible residue in the crystal, Leu73) and the side chain of Lys258 of GGA3 GAT are connected by an orange dotted line. Figure was drawn using PyMOL (http://pymol.sourceforge.net).

Table 1
Distances between the nitrogen atoms of the lysine side chains of C-GAT and the α carbon atom of Leu73 of ubiquitin, in the model structure in Fig. 5

Lysine	*210*	*213*	*249*	*258*	*264*	*294*
Distance (Å)	32.0	24.1	14.3	12.7	24.5	21.5

Leu73 of ubiquitin is the C-terminal residue visible in the crystal.

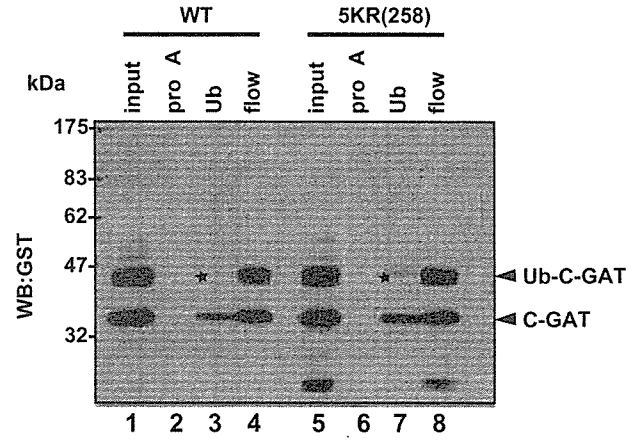

Fig. 6. Ubiquitylated GGA3 prevents further attachment to ubiquitin. The *in vitro* pull-down assay of ubiquitylated GGA3-GAT proteins. Equal amounts of ubiquitylated GGA3-GAT proteins were incubated with Ub- or Protein-A–agarose. The resin was washed, subjected to SDS–PAGE, and detected by Western blot analyses with anti-GST antibody. The supernatants were subjected to incubate with glutathione–Sepharose 4B (lanes 4 and 8). The 25% of input samples were loaded on *input lanes* (lane 1 and 5). Asterisks indicate that ubiquitylated forms of GGA3-GAT could not bind to Ub-agarose.

acids), independently folded motifs; ubiquitin-interacting motif (UIM), ubiquitin-associated (UBA), ubiquitin-conjugating enzyme-like (UBC)/ubiquitin E2 variant (UEV), or Cue1-homologous (CUE) domains [39]. These domains are also referred to as ubiquitin receptors [40]. However, in most cases, little is understood how biochemical interactions are transferred to downstream signals by these ubiquitin-binding proteins. Immediately after ubiquitin-binding abilities were reported, it was generally accepted that ubiquitin receptors are themselves ubiquitylated. Interestingly, the ubiquitylation of ubiquitin receptors requires ubiquitin binding. From our results, all of the GAT mutants that lack ubiquitin binding also inhibit ubiquitylation (Fig. 6). Conversely, a ubiquitin mutant (Ile44Ala) that cannot bind ubiquitin receptors per se cannot be conjugated to GAT domain. Previous reports described that the GAT domain contains two binding sites for ubiquitin [34]. The site 1 centers on leucine 227 and the site 2 centers on leucine 276. The site 1 has a higher affinity for ubiquitin than does site 2. When a ubiquitin was conjugated to the lysine 258 that is close to the site 1, no more ubiquitin can bind to the GGA3 C-GAT. This type of autoinhibition is reminiscent of intramolecular SH2-domain-phosphotyrosine interaction [41]. There has been a strong link between the presence of ubiquitin binding in a protein and its ubiquitylation. Ubiquitin binding and ubiquitylation of ubiquitin receptors are closely coupled and mutually inseparable [42,43]. But so far no ubiquitylation of lysine in the UBD has been reported. This is the first example demonstrating the ubiquitylated lysine resides in the UBD and consequently inhibit further ubiquitin binding. hVPS18 is one of the responsible E3 ubiquitin ligases that directly regulate the ubiquitin binding by conjugating ubiquitin in UBD of GGA3. A major question that has not been answered is to test how E3 hVPS18 is recruited to ubiquitin-binding proteins.

The ubiquitin ligase E3 functions as a monomer or a complex with other cofactors, such as SCF (Skp1/cullin/F-box protein) and the anaphase-promoting complex or cyclosome (APC/C) [35]. But none of the ligase activity has been observed when the catalytic subunit was solely added. Our study showed hVPS18, in the presence of E1 and E2, is sufficient for the *in vitro* ubiquitylation of GGA3, but the modification was significantly enhanced when equal molar of hVPS11 and hVPS16 are mixed. Previous report demonstrated that hVPS18, hVPS11, and hVPS16 constitute a hetero-oligomeric complex in the cytosolic membrane of endosome/lysosome [29]. The aug-

mented ligase-activity implies that the complex formation plays the functionally significant role both *in vivo* and *in vitro*.

In this report, we identified hVPS18 as a ubiquitin ligase (E3) for the monoubiquitylation of GGAs through their ability of ubiquitin-interaction. A number of molecules have been reported to interact with GGA, such as ARF, Rabaptin-5, clathrin, AP-1, and γ-synergin [1,3]. It will be a next issue to address whether these interactions are regulated via monoubiquitylation by hVPS18.

Appendix A. Supplementary data

Supplementary data associated with this article can be found, in the online version, at doi:10.1016/j.bbrc.2006.09.013.

References

[1] J.S. Bonifacino, The GGA proteins: adaptors on the move, Nat. Rev. Mol. Cell. Biol. 5 (2004) 23–32.
[2] I. Hinners, S.A. Tooze, Changing directions: clathrin-mediated transport between the Golgi and endosomes, J. Cell Sci. 116 (2003) 763–771.
[3] K. Nakayama, S. Wakatsuki, The structure and function of GGAs, the traffic controllers at the TGN sorting crossroads, Cell Struct. Funct. 28 (2003) 431–442.
[4] E.C. Dell'Angelica, R. Puertollano, C. Mullins, R.C. Aguilar, J.D. Vargas, L.M. Hartnell, J.S. Bonifacino, GGAs: a family of ADP ribosylation factor-binding proteins related to adaptors and associated with the Golgi complex, J. Cell Biol. 149 (2000) 81–94.
[5] H. Takatsu, K. Yoshino, K. Nakayama, Adaptor gamma ear homology domain conserved in gamma-adaptin and GGA proteins that interact with gamma-synergin, Biochem. Biophys. Res. Commun. 271 (2000) 719–725.
[6] J. Hirst, W.W. Lui, N.A. Bright, N. Totty, M.N. Seaman, M.S. Robinson, A family of proteins with gamma-adaptin and VHS domains that facilitate trafficking between the trans-Golgi network and the vacuole/lysosome, J. Cell Biol. 149 (2000) 67–80.
[7] M. Kawasaki, K. Nakayama, S. Wakatsuki, Membrane recruitment of effector proteins by Arf and Rab GTPases, Curr. Opin. Struct. Biol. (2005).
[8] R. Puertollano, R.C. Aguilar, I. Gorshkova, R.J. Crouch, J.S. Bonifacino, Sorting of mannose 6-phosphate receptors mediated by the GGAs, Science 292 (2001) 1712–1716.
[9] Y. Zhu, B. Doray, A. Poussu, V.P. Lehto, S. Kornfeld, Binding of GGA2 to the lysosomal enzyme sorting motif of the mannose 6-phosphate receptor, Science 292 (2001) 1716–1718.
[10] H. Takatsu, Y. Katoh, Y. Shiba, K. Nakayama, Golgi-localizing, gamma-adaptin ear homology domain, ADP-ribosylation factor-binding (GGA) proteins interact with acidic dileucine sequences within the cytoplasmic domains of sorting receptors through their Vps27p/Hrs/STAM (VHS) domains, J. Biol. Chem. 276 (2001) 28541–28545.
[11] H. Takatsu, K. Yoshino, K. Toda, K. Nakayama, GGA proteins associate with Golgi membranes through interaction between their GGAH domains and ADP-ribosylation factors, Biochem. J. 365 (2002) 369–378.
[12] R. Puertollano, P.A. Randazzo, J.F. Presley, L.M. Hartnell, J.S. Bonifacino, The GGAs promote ARF-dependent recruitment of clathrin to the TGN, Cell 105 (2001) 93–102.
[13] L. Hicke, H.L. Schubert, C.P. Hill, Ubiquitin-binding domains, Nat. Rev. Mol. Cell. Biol. 6 (2005) 610–621.
[14] M.D. Marmor, Y. Yarden, Role of protein ubiquitylation in regulating endocytosis of receptor tyrosine kinases, Oncogene 23 (2004) 2057–2070.
[15] P.P. Di Fiore, S. Polo, K. Hofmann, When ubiquitin meets ubiquitin receptors: a signalling connection, Nat. Rev. Mol. Cell. Biol. 4 (2003) 491–497.
[16] D.J. Katzmann, G. Odorizzi, S.D. Emr, Receptor downregulation and multivesicular-body sorting, Nat. Rev. Mol. Cell. Biol. 3 (2002) 893–905.
[17] Y. Shiba, Y. Katoh, T. Shiba, K. Yoshino, H. Takatsu, H. Kobayashi, H.W. Shin, S. Wakatsuki, K. Nakayama, GAT (GGA and Tom1) domain responsible for ubiquitin binding and ubiquitination, J. Biol. Chem. 279 (2004) 7105–7111.
[18] R. Puertollano, J.S. Bonifacino, Interactions of GGA3 with the ubiquitin sorting machinery, Nat. Cell Biol. 6 (2004) 244–251.
[19] P.M. Scott, P.S. Bilodeau, O. Zhdankina, S.C. Winistorfer, M.J. Hauglund, M.M. Allaman, W.R. Kearney, A.D. Robertson, A.L. Boman, R.C. Piper, GGA proteins bind ubiquitin to facilitate sorting at the trans-Golgi network, Nat. Cell Biol. 6 (2004) 252–259.
[20] R. Mattera, R. Puertollano, W.J. Smith, J.S. Bonifacino, The trihelical bundle subdomain of the GGA proteins interacts with multiple partners through overlapping but distinct sites, J. Biol. Chem. 279 (2004) 31409–31418.
[21] A. d'Azzo, A. Bongiovanni, T. Nastasi, E3 ubiquitin ligases as regulators of membrane protein trafficking and degradation, Traffic 6 (2005) 429–441.
[22] A.A. de Melker, G. van der Horst, J. Calafat, H. Jansen, J. Borst, c-Cbl ubiquitinates the EGF receptor at the plasma membrane and remains receptor associated throughout the endocytic route, J. Cell Sci. 114 (2001) 2167–2178.
[23] S. Polo, S. Sigismund, M. Faretta, M. Guidi, M.R. Capua, G. Bossi, H. Chen, P. De Camilli, P.P. Di Fiore, A single motif responsible for ubiquitin recognition and monoubiquitination in endocytic proteins, Nature 416 (2002) 451–455.
[24] M. Katz, K. Shtiegman, P. Tal-Or, L. Yakir, Y. Mosesson, D. Harari, Y. Machluf, H. Asao, T. Jovin, K. Sugamura, Y. Yarden, Ligand-independent degradation of epidermal growth factor receptor involves receptor ubiquitylation and Hgs, an adaptor whose ubiquitin-interacting motif targets ubiquitylation by Nedd4, Traffic 3 (2002) 740–751.
[25] T.K. Sato, P. Rehling, M.R. Peterson, S.D. Emr, Class C Vps protein complex regulates vacuolar SNARE pairing and is required for vesicle docking/fusion, Mol. Cell 6 (2000) 661–671.
[26] M.R. Peterson, S.D. Emr, The class C Vps complex functions at multiple stages of the vacuolar transport pathway, Traffic 2 (2001) 476–486.
[27] V. Poupon, A. Stewart, S.R. Gray, R.C. Piper, J.P. Luzio, The role of mVps18p in clustering, fusion, and intracellular localization of late endocytic prganelles, Mol. Bio. Cell 14 (2003) 4015–4027.
[28] S.C. Richardson, S.C. Winistorfer, V. Poupon, J.P. Luzio, R.C. Piper, Mammalian late vacuole protein sorting orthologues participate in early endosomal fusion and interact with the cytoskeleton, Mol. Biol. Cell 15 (2004) 1197–1210.
[29] B.Y. Kim, H. Kramer, A. Yamamoto, E. Kominami, S. Kohsaka, C. Akazawa, Molecular characterization of mammalian homologues of class C Vps proteins that interact with syntaxin-7, J. Biol. Chem. 276 (2001) 29393–29402.
[30] S. Caplan, L.M. Hartnell, R.C. Aguilar, N. Naslavsky, J.S. Bonifacino, Human Vam6p promotes lysosome clustering and fusion in vivo, J. Cell Biol. 154 (2001) 109–122.
[31] S. Yogosawa, S. Hatakeyama, K.I. Nakayama, H. Miyoshi, S. Kohsaka, C. Akazawa, Ubiquitylation and degradation of polo-like kinase SNK by hVPS18, a RING-H2 type ubiquitin ligase, J. Biol. Chem. 280 (2005) 41619–41627.
[32] S.L. Miller, E. Malotky, J.P. O'Bryan, Analysis of the role of ubiquitin-interacting motifs in ubiquitin binding and ubiquitylation, J. Biol. Chem. 279 (2004) 33528–33537.

[33] S.C. Shih, G. Prag, S.A. Francis, M.A. Sutanto, J.H. Hurley, L. Hicke, A ubiquitin-binding motif required for intramolecular monoubiquitylation, the CUE domain, EMBO J. 22 (2003) 1273–1281.
[34] M. Kawasaki, T. Shiba, Y. Shiba, Y. Yamaguchi, N. Matsugaki, N. Igarashi, M. Suzuki, R. Kato, K. Kato, K. Nakayama, S. Wakatsuki, Molecular mechanism of ubiquitin recognition by GGA3 GAT domain, Genes Cells 10 (2005) 639–654.
[35] A.M. Weissman, Themes and variations on ubiquitylation, Nat. Rev. Mol. Cell. Biol. 2 (2001) 169–178.
[36] R.C. Aguilar, B. Wendland, Ubiquitin: not just for proteasomes anymore, Curr. Opin. Cell Biol. 15 (2003) 184–190.
[37] Y. Katoh, Y. Shiba, H. Mitsuhashi, Y. Yanagida, H. Takatsu, K. Nakayama, Tollip and Tom1 form a complex and recruit ubiquitin-conjugated proteins onto early endosomes, J. Biol. Chem. 279 (2004) 24435–24443.
[38] M. Yamakami, T. Yoshimori, H. Yokosawa, Tom1, a VHS domain-containing protein, interacts with tollip, ubiquitin, and clathrin, J. Biol. Chem. 278 (2003) 52865–52872.
[39] K. Haglund, I. Dikic, Ubiquitylation and cell signaling, EMBO J. 24 (2005) 3353–3359.
[40] K. Haglund, P.P. Di Fiore, I. Dikic, Distinct monoubiquitin signals in receptor endocytosis, Trends Biochem. Sci. 28 (2003) 598–603.
[41] J. Kuriyan, D. Cowburn, Modular peptide recognition domains in eukaryotic signaling, Annu. Rev. Biophys. Biomol. Struct. 26 (1997) 259–288.
[42] M. Bienko, C.M. Green, N. Crosetto, F. Rudolf, G. Zapart, B. Coull, P. Kannouche, G. Wider, M. Peter, A.R. Lehmann, K. Hofmann, I. Dikic, Ubiquitin-binding domains in Y-family polymerases regulate translesion synthesis, Science 310 (2005) 1821–1824.
[43] D. Hoeller, N. Crosetto, B. Blagoev, C. Raiborg, R. Tikkanen, S. Wagner, K. Kowanetz, R. Breitling, M. Mann, H. Stenmark, I. Dikic, Regulation of ubiquitin-binding proteins by monoubiquitination, Nat. Cell Biol. 8 (2006) 163–169.
[44] T. Shiba, M. Kawasaki, H. Takatsu, T. Nogi, N. Matsugaki, N. Igarashi, M. Suzuki, R. Kato, K. Nakayama, S. Wakatsuki, Molecular mechanism of membrane recruitment of GGA by ARF in lysosomal protein transport, Nat. Struct. Biol. 10 (2003) 386–393.

Neuroscience 141 (2006) 1861–1869

ABERRANT TRAFFICKING OF A PROTEOLIPID PROTEIN IN A MILD PELIZAEUS-MERZBACHER DISEASE

S. KOIZUME,[a,c,d] S. TAKIZAWA,[a,c] K. FUJITA,[b] N. AIDA,[b] S. YAMASHITA,[a] Y. MIYAGI[d] AND H. OSAKA[a,c]*

[a]*Division of Neurology, Clinical Research Institute, Kanagawa Children's Medical Center, Mutsukawa 2-138-4, Minami-ku, Yokohama 232-8555, Japan*

[b]*Division of Radiology, Clinical Research Institute, Kanagawa Children's Medical Center, Yokohama 232-855, Japan*

[c]*Information and Cellular function, PRESTO, Japan Science and Technology Corporation, Kawaguchi, Saitama 332-0012, Japan*

[d]*Molecular Pathology and Genetics Division, Kanagawa Cancer Center Research Institute, Yokohama 241-0815, Japan*

Abstract—Pelizaeus-Merzbacher disease (PMD) is a rare X-linked leukodystrophy caused by proteolipid protein 1 (*PLP1*) gene mutations. Previous studies indicated that proteolipid proteins (PLPs) with disease-associated mutations are misfolded and trapped in the endoplasmic reticulum (ER) during transportation to the cell surface, which eventually leads to oligodendrocyte cell death in PMD. Here we report a PMD patient with a very mild phenotype carrying a novel mutation (485G→T) in exon 4 of the *PLP1* gene that causes a $Trp^{162}Leu$ substitution in the protein. We also investigated intracellular trafficking of this mutant PLP in COS-7 cells. Transiently transfected mutant PLP^{W162L} fused to an enhanced green fluorescent protein (EGFP) or a short peptide tag was not carried to the plasma membrane. However, in contrast to previous studies, this mutant PLP was not retained in the ER, indicating an escape of the newly translated protein from the quality control machinery. We also found that the mutant PLP accumulated in the nuclear envelope (NE) in a time-dependent manner. This mutant PLP, with its distribution outside the ER and a very mild phenotype, supports the idea that accumulation of misfolded mutant protein in the ER causes the severe phenotype of PMD.

Key words: Pelizaeus-Merzbacher disease, proteolipid protein, intracellular trafficking, unfolded protein response.

Pelizaeus-Merzbacher disease (PMD) and its allelic disorder, spastic paraplegia type 2, (SPG2) are X-linked recessive disorders associated with aberration of the proteolipid protein 1 (*PLP1*) gene. Proteolipid protein (PLP) is composed of 276 amino acid residues and predominantly expressed in oligodendrocytes of the CNS. As an integral membrane protein necessary for stabilization and maintenance of the myelin sheath (Inoue, 2005), it comprises up to ~50% of total myelin protein (Inoue, 2005). PMD is generally classified according to clinical or pathological features into mild (classical) or severe (connatal) forms (Griffiths et al., 1998; Inoue, 2005). A milder form of this disorder caused by mutations of the *PLP1* gene is known as spastic paraplegia (SPG) 2 (Griffiths et al., 1998; Inoue, 2005). Although the common feature of PMD is hypomyelination (Roussel et al., 1987; Schneider et al., 1992; Kagawa et al., 1994; Readhead et al., 1994) in the CNS, degeneration of oligodendrocytes is also characteristic in severe cases (Gow et al., 1998; Cerghet et al., 2001).

Various types of mutations of the *PLP1* gene, including exonic or intronic mutations, duplication, or deletion of the entire gene are responsible for PMD (Griffiths et al., 1998; Inoue, 2005). Patients carrying duplicated alleles show demyelination and patients with no *PLP1* alleles show only very mild clinical symptoms (Inoue, 2005), suggesting that the disease is caused by a toxic gain-of-function. It is known that exonic point mutations are present in 10~25% of reported PMD cases with variations in disease severity (Boespflug-Tanguy et al., 1994). DM20, an isoform of PLP whose role in the CNS is unclear, is produced from a *PLP1* transcript that lacks the second half of exon 3. Mutations in this region usually cause mild symptoms consistent with SPG. However, mutations in other coding regions of the *PLP1* gene usually cause severe mental retardation and deficits in motor function (i.e. loss of head control and sitting) with diffuse T2 elongation in magnetic resonance imaging (MRI) and disappearance of the II-V waves in auditory brain responses. Various intracellular trafficking studies have been conducted with the PLPs resulting from point mutations of the *PLP1* gene (Gow et al., 1994a,b; Thomson et al., 1997; Ghandour et al., 2002). Previous *in vitro* transfection studies in non-glial cells indicated that various mutant PLPs, irrespective of associated disease severity, are trapped in the endoplasmic reticulum (ER) immediately after translation, and thereby not transported to the plasma membrane (Gow et al., 1994b; Gow and Lazzarini, 1996; Thomson et al., 1997). Several studies have suggested that ER-retention of mutant PLP/DM20s causes oligodendrocytic programmed cell death (Gow et al., 1998; Cerghet et al., 2001; Southwood et al., 2002). An unfolded protein response (UPR) followed by caspase activation-mediated apoptosis is a plausible mechanism given the ER stress induced by accumulation of mutant

*Correspondence to: H. Osaka, Division of Neurology, Clinical Research Institute, Kanagawa Children's Medical Center, Mutsukawa 2-138-4, Minami-ku, Yokohama, 232–8555, Japan. Tel: +81-45-711-2351; fax: +81-45-721-3324.
E-mail address: kcmc_ho@cameo.plala.or.jp (H. Osaka).

Abbreviations: BiP, 78-kDa glucose regulated protein/immunoglobulin heavy chain binding protein; CFTR, cystic fibrosis transmembrane conductance regulator; DYT1 dystonia, torsion dystonia type 1; EGFP, enhanced green fluorescent protein; ER, endoplasmic reticulum; MRI, magnetic resonance imaging; NE, nuclear envelope; PLP, proteolipid protein; *PLP1 gene*, proteolipid protein 1 gene; PMD, Pelizaeus-Merzbacher disease; SPG, spastic paraplegia; UPR, unfolded protein response.

0306-4522/06$30.00+0.00
doi:10.1016/j.neuroscience.2006.05.067

PLP/DM20s in the ER (Gow and Sharma, 2003). In case of PMDs due to *PLP1*-gene duplication, demyelination is thought to be caused by perturbed protein transport such as impaired raft membrane trafficking (Simons et al., 2002). Involvement of UPR is unlikely because activation of caspase-12 was not detected in CNS of PLP-overexpressor mice (Cerghet et al., 2001).

In this study, we present a PMD patient with a very mild phenotype who could stand and speak a few words at 20 months, displayed almost complete myelination in both T1 and T2 images of MRI, and whose V waves were all detectable in auditory brain-stem response. We sequenced the patient's *PLP1* exons, and found a novel missense mutation in codon 162 (485G→T, $Trp^{162}Leu$). We further analyzed the effect of the mutation on trafficking of PLP in cells using confocal microscopy. In contrast to the results of previous studies, we found that PLP^{W162L} transiently expressed in COS-7 cells as a fusion protein of either enhanced green fluorescent protein (EGFP) or a FLAG peptide tag is not retained in the ER after synthesis and does not reach the cell surface. Furthermore, we found that PLP^{W162L}-EGFP accumulates in the nuclear envelope (NE). These data together with the very mild phenotype of our patient, similar to *PLP1*-null patients, support the idea that the UPR plays a crucial role in PMD.

EXPERIMENTAL PROCEDURES

Patient

This 3-year-old boy was born uneventfully at full term to unrelated Japanese parents. He was born with a body weight of 2990 g and an Apgar score of 9/9 at 1 and 5 min. No stridor or nystagmus was noted. He gained head control at 4 months, could sit without support at 14 months and could stand at 20 months, when he was referred to our hospital for evaluation of developmental delay. He could speak a few words and stand with support. Nystagmus was observed when he gazed laterally. He exhibited left hemiparesis with his upper extremities rotated inwardly and flexed at the elbow. His muscle tone was hypotonic with all extremities displaying exaggerated tendon reflexes and bilateral extensor plantar responses. No cerebellar signs or involuntary movements were observed. His developmental milestones were 9 months for motor function, 10 months for language understanding and 18 months for fine motor movements. Upon routine laboratory examination, no biochemical abnormalities were noted in serum ammonia, lactate and pyruvate levels, very long chain fatty acids and lysosomal enzymes. Myelin basic protein was not detected in the CSF. Nerve conduction velocities and electromyographic studies were all normal. Auditory brain-stem response elicited normal latencies with normal detectable V waves. MRI revealed a completion of myelination and a subependymal cyst in the right frontal region in the T1 signal. Myelination was incomplete in the insula and optic radiation in the T2 signal (Fig. 1).

Genomic DNA sequencing

Genomic DNA from this patient was prepared from white blood cells using the Wizard Genomic DNA purification kit (Promega, Madison, WI, USA). PCR of seven exons and promoter regions of the *PLP1* gene was performed as previously described (Osaka et al., 1999). Subsequent sequencing analyses of the PCR fragments were performed by direct sequencing using the Big Dye Terminators v1.1 Cycle Sequencing kit (Applied Biosystems, Foster City, CA, USA).

Cell culture and transfection

COS-7 cells were cultured in Dulbecco's modified Eagle's medium (DMEM) (Gibco BRL, Carlsbad, CA, USA) supplemented with 10% fetal bovine serum (Gibco BRL), 2 mM glutamine (Gibco BRL), and 100 U/ml penicillin/streptomycin (Gibco BRL) at 37 °C under humidified 5% CO_2 atmosphere. This cell line is non-glial in origin but does not express endogenous PLP and has often been used for intracellular trafficking studies of PLPs. Transient transfection of all plasmid constructs used in this study was performed using Lipofectamine™ 2000 (Invitrogen, Carlsbad, CA, USA) according to the manufacturer's protocol.

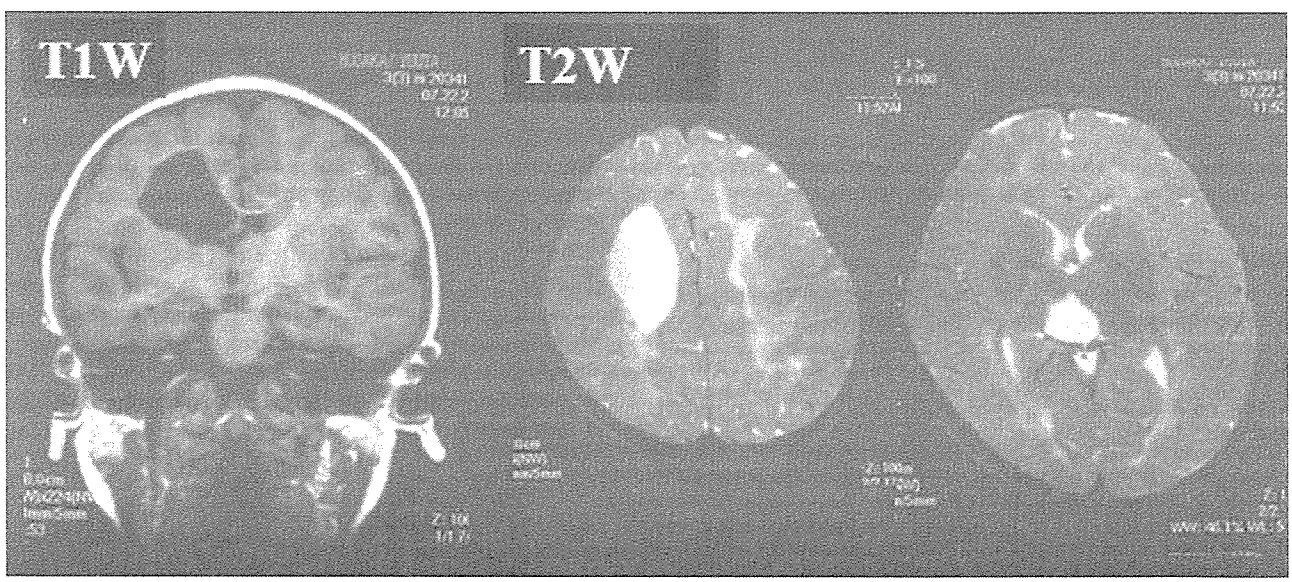

Fig. 1. Magnetic resonance images at two y. T1-weighted image shows a subependymal cyst in the right frontal region. Myelination is complete in the T1-weighted image. Myelination is incomplete in the optic radiation and internal capsule in the T2-weighted image.

Plasmid construction

Full-length cDNA of human *PLP1* (positions 119–949, accession no. M27110) was amplified by PCR and cloned into the pEGFP-N1 vector (Clontech, Mountain View, CA, USA) at the *EcoRI*/*BamHI* site to produce pPLP-EGFP. We took advantage of this vector, due to its strong gene expression driven by a CMV promoter, to recapitulate the high level of PLP expression in oligodendrocytes (Gow, 2003). PLP^{W162L} and its negative or positive ER retention controls, wild-type PLP (PLP^{WT}) and $Ala^{242}Val$ (myelin synthesis deficient) mutant PLP (PLP^{msd}), respectively, were designed to fuse to an EGFP at its C-terminal end for direct detection in live cells. A construct for expression of wild-type PLP fused to a FLAG tag was derived from $pPLP^{WT}$-EGFP. A plasmid was designed to express PLP-FLAGs by inserting a FLAG tag nucleotide sequence between the PLP and EGFP sequences and halting translation before synthesis of the EGFP moiety was initiated. A double-stranded oligonucleotide consisting of a FLAG sequence with a stop codon at the 3′-end was ligated into pPLP-EGFP at the *BamHI* site to produce pPLP-FLAG-EGFP. Bacterial colonies transformed by ligated plasmids with the desired FLAG sequence orientation were selected by colony PCR. The resulting plasmid constructs were propagated by standard procedures and purified using a QIA filter plasmid kit (Qiagen, Germantown, MD, USA). Site-directed mutagenesis of the pPLP-EGFP and pPLP-FLAG constructs was performed using a QuikChange™ site-directed mutagenesis kit (Stratagene, La Jolla, CA, USA) according to the manufacturer's protocol. Primers used for strand synthesis were 5′-CCTGACCGTTGTGTTGCTCCTGGTG-3′ and 5′-CACCAGGAGCAACACAACGGTCAGG-3′ (for the Trp162Leu conversion), and 5′-CCTGTTTATTGCTGTATTTGTGGGGG-3′ and 5′-CCCCCACAAATACAGCAATAAACAGG-3′ (for the Ala242Val conversion). Mutant plasmid constructs were confirmed by nucleotide sequencing using the BigDye™ Terminator Cycle Sequencing Ready Reaction kit (Applied Biosystems).

Analyses of subcellular localization of PLPs in living cells

Cultured cells, transfected with pPLP-EGFPs alone or with both pPLP-EGFP and pDsRed2-ER (Clontech), were directly examined for confocal microscopy. Subcellular localization of PLP-EGFPs was analyzed by laser scanning microscopy using a model LSM5 PASCAL system (Carl Zeiss Microimaging, Inc., Thornwood, NY, USA).

Immunofluorescence staining

Cells were seeded on four-well chamber glass slides (Falcon, Franklin Lakes, NJ, USA) and cultured for 20 or 40 h. After 20 h of transient transfection of pPLP-FLAGs or pPLP-EGFPs, cells were briefly washed once with PBS and fixed with 4% paraformaldehyde in PBS for 10 min. Fixed cells were washed twice with PBS and permeabilized with 0.1% Triton X-100 (Sigma, St. Louis, MO, USA) in PBS for 10 min. Cells were washed and incubated with 3% normal goat serum (Nichirei, Tokyo, Japan) for 15 min to reduce non-specific binding of antibodies and then incubated for 1 h with primary antibodies of anti-FLAG (1:100; F7425, Sigma), anti-KDEL (BiP, 78-kDa glucose regulated protein/immunoglobulin heavy chain binding protein) (1:100; SPA-827, Stressgen, Ann Arbor, MI, USA), or anti-laminA (1:100; sc-20680, Santa Cruz Biotechnology, Santa Cruz, CA, USA) diluted with blocking reagent containing 0.1% Triton X-100. After washing (10 min×3) with PBS, cells were finally incubated for 1 h with secondary antibodies conjugated with Alexa Fluor 488 or 546 dyes (Molecular Probes, Carlsbad, CA, USA) diluted with blocking reagent. Labeled cells were washed and sealed using the SlowFade® antifade kit (Molecular Probes). All steps were carried out at RT. Subcellular localization of proteins was analyzed by confocal microscopy as described above.

RESULTS

Sequencing of exons of the PLP1 gene and plasmid construction

By direct sequencing of the patient's *PLP1* gene exons and a promoter region, we found a novel missense mutation (485G→T, $Trp^{162}Leu$) in codon 162, in which another missense mutation (484T→C, $Trp^{162}Arg$) had been previously reported in a severe PMD patient (Hudson et al., 1989). No other sequence alterations were found and this mutation was not detected in more than 200 alleles. Furthermore, amino acid sequences are completely conserved within vertebrates and no protein polymorphism is known in the PLP (Inoue, 2005). Therefore, the $Trp^{162}Leu$ substitution appears to cause PMD. Previous transfection studies showed that all PLPs with a disease-associated point mutation were localized in the perinuclear ER, probably due to misfolding.

Subcellular localization of PLP^{W162L}-EGFP transiently expressed in COS-7 cells

We first estimated the subcellular localization of EGFP in COS-7 cells. After 40 h of transient cDNA transfection, non-fused EGFP was distributed within the cytoplasm including the nucleus of cells (Fig. 2A) as reported previously (Boucher et al., 2002). PLP^{WT}-EGFP was distributed throughout the cell body except the nucleus (Fig. 2B) and extended to the periphery of cells (Fig. 2B, arrows), suggesting insertion in the plasma membrane as previously shown by immunostaining of transfected HEK293 cells with a conformation specific O10 antibody (Boucher et al., 2002). We confirmed the extension of PLP^{WT}-EGFP to the cell surface by overlaying its fluorescence image with a light field micrograph (Fig. 3). PLP^{msd}-EGFP, as expected, accumulated in the perinuclear region in most cells and was not transported to the cell surface (Fig. 2C). PLP^{W162L}-EGFP also accumulated in the perinuclear region like the *msd* mutant but was not found at the cell periphery where the wild-type PLP was observed (Fig. 2D, arrowheads), suggesting that arrival at the cell surface is unlikely. The absence of PLP^{W162L}-EGFP in the plasma membrane was further confirmed by overlaying the fluorescence image with its light field micrograph (Fig. 3). In addition, a $Trp^{162}Leu$ mutant localization characteristic for that of the perinuclear rim was unexpectedly detected in many cells (Fig. 2D, arrows).

Subcellular localization of PLP^{W162L}-EGFP transiently co-expressed with DsRed2-ER

We performed time-lapse monitoring of the subcellular localization of wild-type and mutant PLP-EGFPs. As a marker for ER, we used the red-fluorescent DsRed2-ER protein, in which the ER retention signal peptide of calreticulin was anchored. After 15, 24, and 40 h of co-transfection with pPLP-EGFPs and pDsRed2-ER, presence of wild-type and mutant PLP-EGFPs in the ER was directly exam-

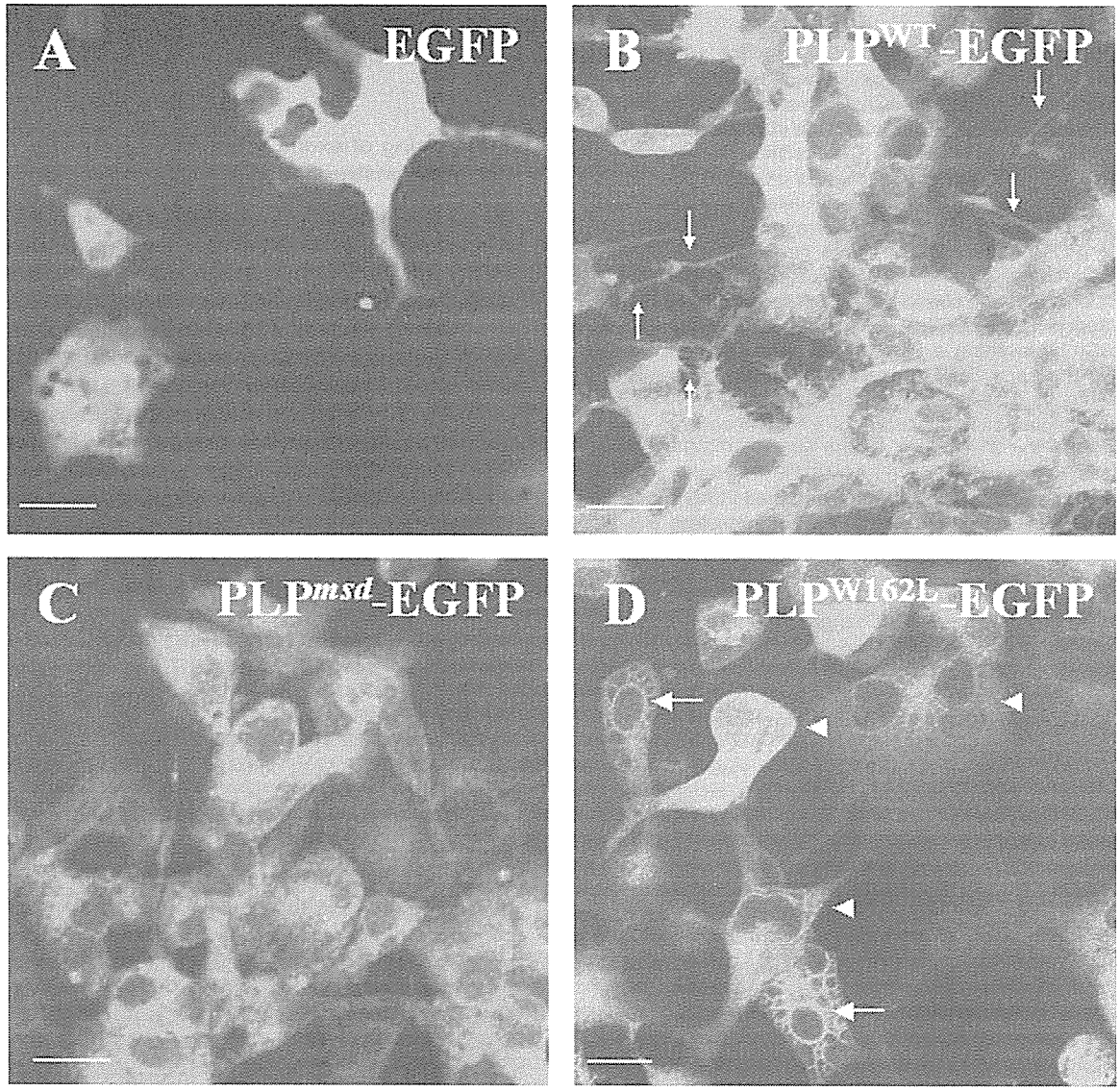

Fig. 2. Live-cell images of wild-type or mutant PLP-EGFPs transiently transfected in COS-7 cells. Confocal laser scanning images were collected 40 h after transfection with EGFP (A), PLP^{WT}-EGFP (B), PLP^{msd}-EGFP (C), or PLP^{W162L}-EGFP (D). Arrows in B are indicative of wild-type PLP-EGFP in the cell periphery. Arrowheads and arrows in D are indicative of PLP^{W162L}-EGFP localizations in the perinuclear region and at the perinuclear rim, respectively. Each panel is a representative, single optical slice image from independent, duplicate experiments. Scale bars=20 μm.

ined (Fig. 4). The negative control experiment revealed that EGFP alone did not colocalize with DsRed2-ER at 15 and 24 h (Fig. 4A) although some colocalization, seen as orange fluorescence, was detected at 40 h (Fig. 4A). Much of the PLP^{WT}-EGFP was found in the cytoplasmic region (Fig. 4B, green color around yellow colored region), suggesting that wild-type PLP passed through the ER and was transported to the cytoplasm. However, yellow fluorescence was found in the perinuclear regions of PLP^{WT}-EGFP transfected cells in the three time periods and is evidence that wild-type PLP was localized to the ER throughout the time course (Fig. 4B, arrows). In cells co-transfected with the positive ER-retention control PLP^{msd}-EGFP, the majority of the fluorescence is localized in the perinuclear region and is visible as a yellow color due to colocalization with the ER in most cells at all time points examined (Fig. 4C). Unlike the wild-type protein, we did not find much green fluorescing *msd* mutant protein *around* the ER, confirming its entrapment *in* the ER. These results also show that the overall characteristics of intracellular trafficking of both EGFP-tagged PLP^{WT} and PLP^{msd} are not altered throughout the time-course in COS-7 cells.

The PLP mutant, PLP^{W162L}-EGFP (green fluorescence) was found largely in cytoplasmic regions beyond the ER (Fig. 4D) at all time points. At 15 and 24 h post transfection, some PLP^{W162L}-EGFP was found in the ER (yellow fluorescence) (Fig. 4D, arrows). This suggests a passage of this mutant, similar to that of the wild-type protein, through the ER quality control mechanism. Surprisingly however, PLP^{W162L}-EGFP expressed 40 h after transfection did not overlap with, and was clearly distinct from, the ER in most cells (Fig. 4D and Supplement 1), but

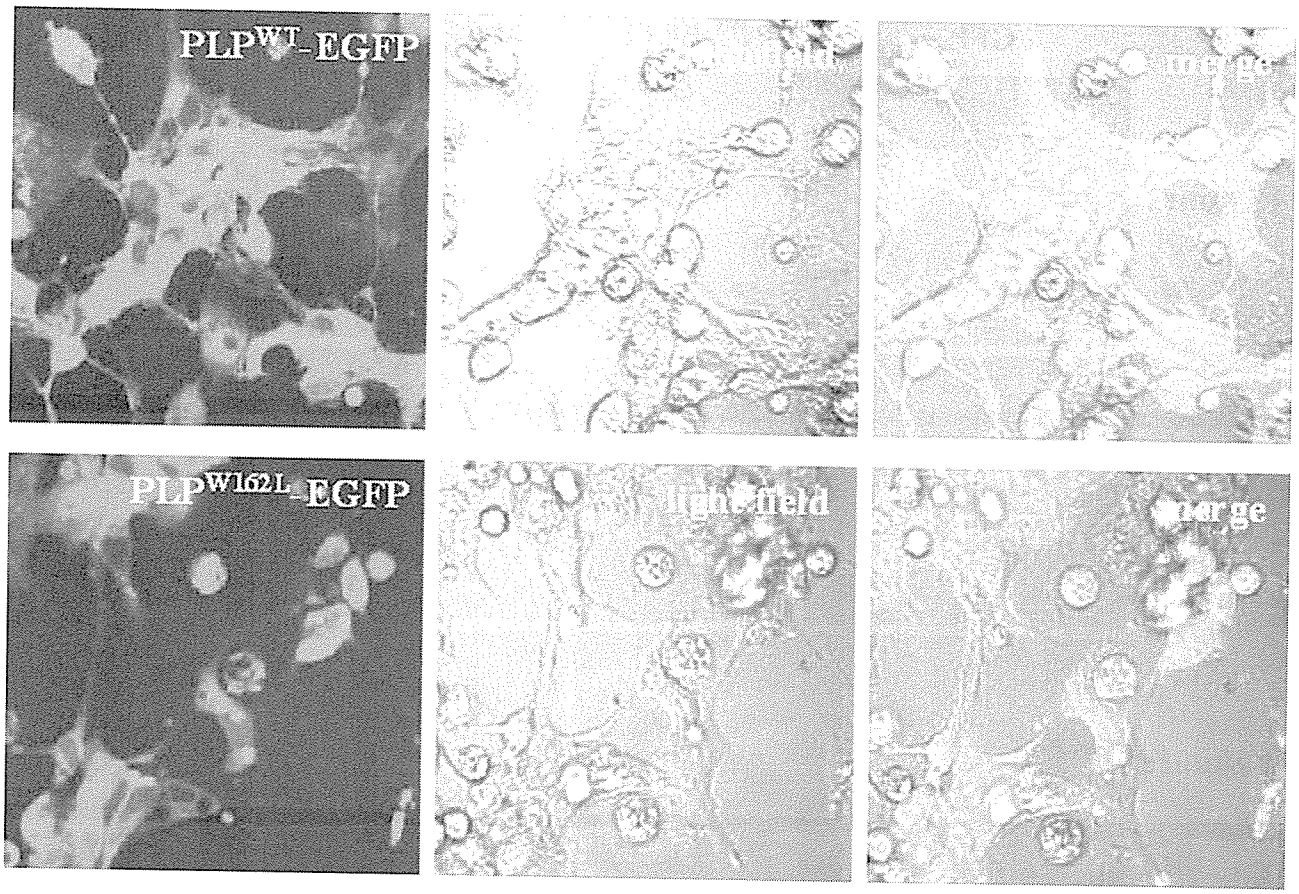

Fig. 3. Intracellular distribution of PLP^{WT}-EGFP and PLP^{W162L}-EGFP in COS-7 cells. Image of wild-type or the Trp^{162}Leu mutant PLP-EGFP visualized by laser scanning microscopy is overlaid with its light field micrograph.

was also localized to the perinuclear rim (Fig. 4D, an arrowhead and Supplement 1).

Detailed analyses of subcellular localization of PLP^{W162L}-EGFP accumulating in the perinuclear region

Following our discovery that PLP^{W162L}-EGFP expressed in COS-7 cells does not colocalize with an ER marker but accumulates at the perinuclear rim (Fig. 2D, arrows), we suspected that the Trp^{162}Leu mutant localizes to the NE. The NE was recently proposed to be a site of action of torsinA mutants, resulting in a CNS disorder known as torsion dystonia type 1 (DYT1 dystonia) (Gonzalez-Alegre and Paulson, 2004; Goodchild and Dauer, 2004; Naismith et al., 2004). Thus, we next tested whether the Trp^{162}Leu mutant resides in the NE by immunostaining COS-7 cells with an antibody against the NE protein, laminA, 40 h after transient transfection. Immunofluorescence revealed that the Trp^{162}Leu mutant accumulating at the perinuclear rim colocalizes with laminA in many cells (Fig. 5A, arrows and Supplement 2), suggesting that PLP^{W162L}-EGFP concentrates in the NE. By contrast, neither PLP^{WT}-EGFP (Fig. 5B) nor PLP^{msd}-EGFP (Fig. 5C) accumulated in the NE in most cells, although weak yellow fluorescence due to NE colocalization was occasionally seen (Fig. 5B and C, arrows). These results are consistent with the previously reported immunofluorescence studies showing that proteins retained in the ER, such as wild-type torsinA, have some colocalization with the NE (Gonzalez-Alegre and Paulson, 2004; Goodchild and Dauer, 2004).

Subcellular localization of PLP^{W162L}-FLAG transiently expressed in COS-7 cells

The absence of transiently expressed PLP^{W162L}-EGFP in the ER could also possibly be due to the large, artificially linked EGFP moiety. Therefore, we tested whether PLP^{W162L} tethered to a small peptide tag (FLAG), instead of EGFP, is retained in the ER after transfection. Twenty hours or 40 h after transient transfection in COS-7 cells, PLP-FLAGs were detected by immunofluorescence staining and confocal microscopy. Grp78/BiP immunostaining was used as an ER marker. Transiently transfected PLP^{WT}-FLAG was distributed in the cytosol (Fig. 6A) and weakly colocalized with BiP (Fig. 6A, arrows), confirming that there is no significant accumulation in the ER, similar to the EGFP-fused protein. As expected, PLP^{msd}-FLAG immunofluorescence was found in the perinuclear region and overlapped with BiP (Fig. 6B). Neither PLP^{WT}-FLAG nor PLP^{msd}-FLAG accumulations were detected at the perinuclear rim (Fig. 6A and B). Some PLP^{W162L}-FLAGs were also found

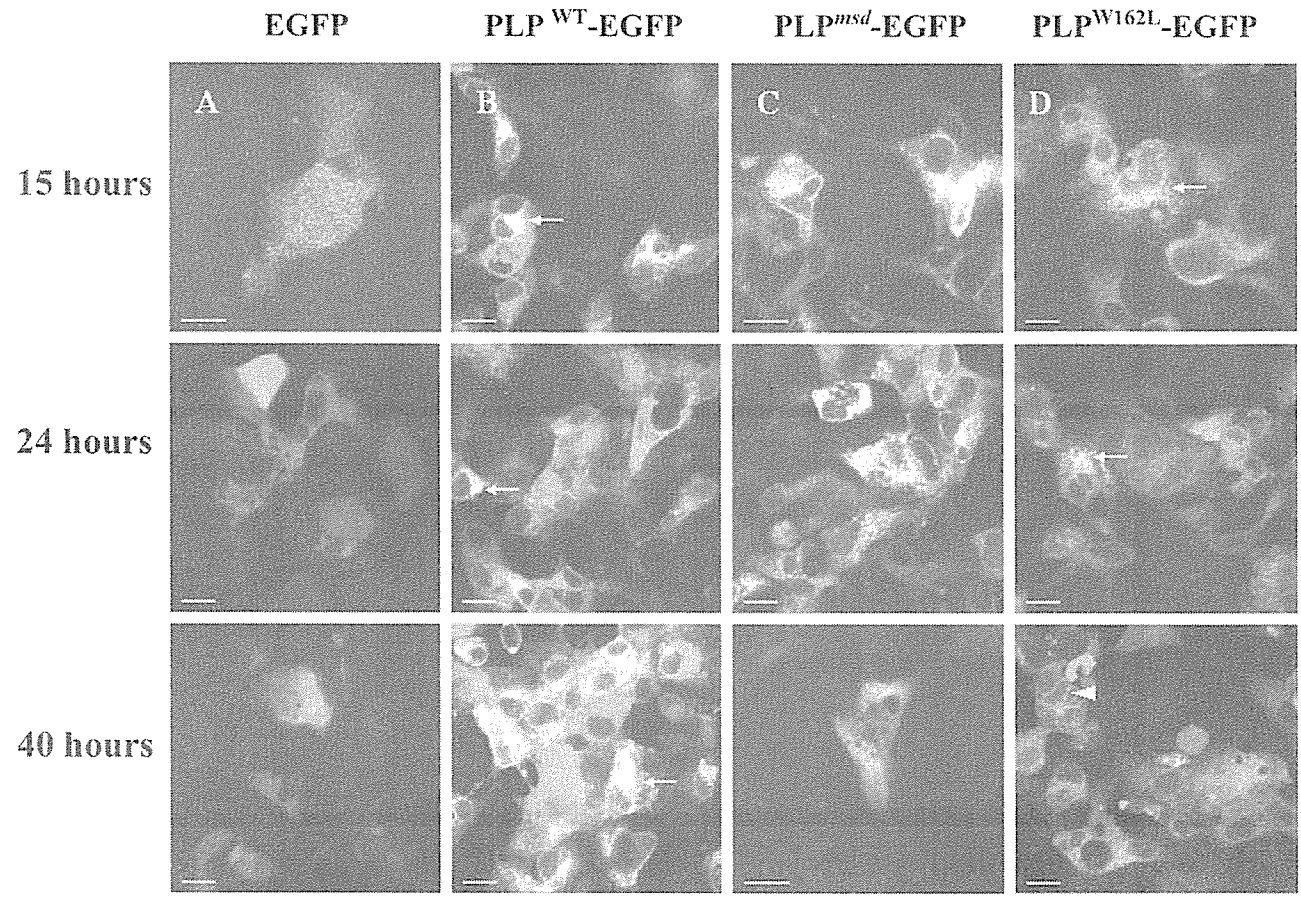

Fig. 4. Time-course monitoring of the subcellular localization of PLP-EGFPs in live cells. COS-7 cells were transiently transfected with EGFP (A), PLP^{WT}-EGFP (B), PLP^{msd}-EGFP (C), or PLP^{W162L}-EGFP (D) and visualized (green) by laser scanning microscopy. ER was simultaneously stained (red) by co-transfection of DsRed2-ER. Confocal images were collected at the indicated time points after transfection. Panels depicted are representative, single optical slices of three independent experiments. Yellow to orange color is indicative of colocalized PLP-EGFPs and ER. Arrows are indicative of ER localizations of wild-type or $Trp^{162}Leu$ mutant PLP-EGFPs. The arrowhead in D is indicative of perinuclear rim localization of PLP^{W162L}-EGFP. Scale bars=20 μm.

localized in the perinuclear region and weakly colocalized with BiP (Fig. 6C, an arrow). Perinuclear rim localization of this mutant PLP was occasionally seen (Fig. 6C, inset). However, PLP^{W162L}-FLAG colocalized only partially with BiP (Fig. 6C, an arrowhead) in many cells and distributed in the cytosol similar to the wild-type PLP, indicating detachment of the $Trp^{162}Leu$ mutant from the ER after translation. These data exclude the possibility that adding EGFP changed the subcellular localization of PLP.

DISCUSSION

The fact that the majority of *PLP1* point mutations cause more severe dysmyelinating disease than those caused by *null* mutations (i.e. deletions and truncations within exon 1) suggests that the profound dysmyelination resulting from *PLP1* point mutations and overexpressions probably arises not from absence of functional protein, but rather from the cytotoxic effect of mutant proteins. PLPs translated from the transfected *PLP1* cDNA with disease-associated point mutations are known to be trapped in the ER of glial tissue (Southwood et al., 2002) and non-glial cells (Gow et al., 1994b; Gow and Lazzarini, 1996; Thomson et al., 1997) in the process of being transported to the cell surface. It was assumed that those mutations led to misfolding of PLPs during translation in oligodendrocytes of patients. Unfolded PLPs are thought to accumulate in the ER and then are transferred to the cytosol for ER-associated protein degradation (ERAD) to prevent resulting cytotoxic effects (Kaufman, 2002; Gow and Sharma, 2003). Excessive misfolded PLPs not processed by degradation could result in the death of oligodendrocytes by UPR-mediated apoptotic mechanisms (Kaufman, 2002).

We found a novel missense mutation (485G→T, $Trp^{162}Leu$) in exon 4 of the *PLP1* gene of a patient suspected of having PMD. We further showed that this disease-associated mutant PLP fused to an EGFP or a FLAG tag and transfected in COS-7 cells is not retained in the ER but accumulates in the perinuclear region. The data suggest that PLP^{W162L} escapes from trapping by the quality control machinery for newly synthesized proteins in the ER. This is in contrast to the results of previous *in vitro*

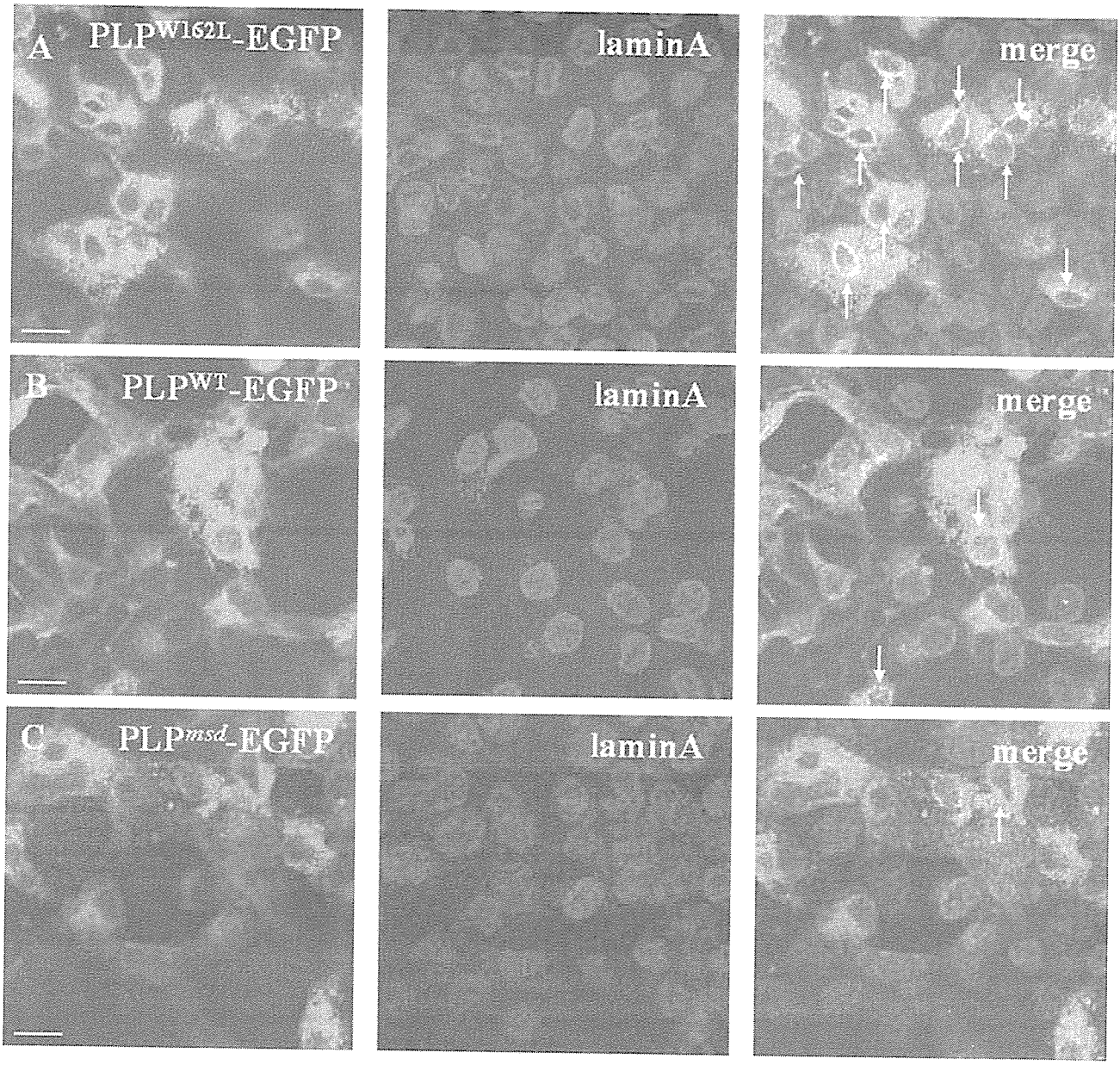

Fig. 5. Presence of PLP^{W162L}-EGFP in the NE. Forty hours after transient transfection with PLP^{W162L}-EGFP (A), PLP^{WT}-EGFP (B), or PLP^{msd}-EGFP (C), paraformaldehyde-fixed COS-7 cells were immunofluorescently stained with an antibody against the NE protein, laminA (red: Alexa 546). Yellow fluorescence is indicative of colocalized PLP^{W162L}-EGFP and NE. Panels are representative single confocal images of independent, triplicate experiments. Scale bars=20 μm.

trafficking studies showing that many transfected PLPs with naturally occurring point mutations are accumulated in the ER directly after translation (Gow et al., 1994b; Gow and Lazzarini, 1996; Thomson et al., 1997). However, it has been reported that the *partially* unfolded cystic fibrosis transmembrane conductance regulator (CFTR) protein expressed in BHK cells is not trapped in the ER whereas *fully* misfolded CFTR is retained in the ER during trafficking toward the cell surface (Sharma et al., 2004). Partially misfolded CFTR was shown to reach the cell surface but was short-lived because of degradation due to inefficient recycling at the cell surface (Gentzsch et al., 2004; Sharma et al., 2004). The lack of PLP^{W162L}-retention in the ER may be due to a similar mild alteration in its three-dimensional structure, thereby enabling it to escape from the quality control of the secretory pathway.

There was a time-dependence of the subcellular localization of PLP^{W162L}-EGFP in COS-7 cells although wild-type and *msd* mutant protein showed no such correlations. Distribution of PLP^{W162L}-EGFP in cells at early time points (15 and 24 h) after transfection (Fig. 4D) was similar to that of wild-type protein (Fig. 4B). Some observations of PLP^{W162L}-EGFPs localized in the ER were probably due to PLP molecules under translation as previously reported for wild-type PLP (Gow et al., 1994a). However, 40 h after transfection, almost no PLP^{W162L} was found localized to

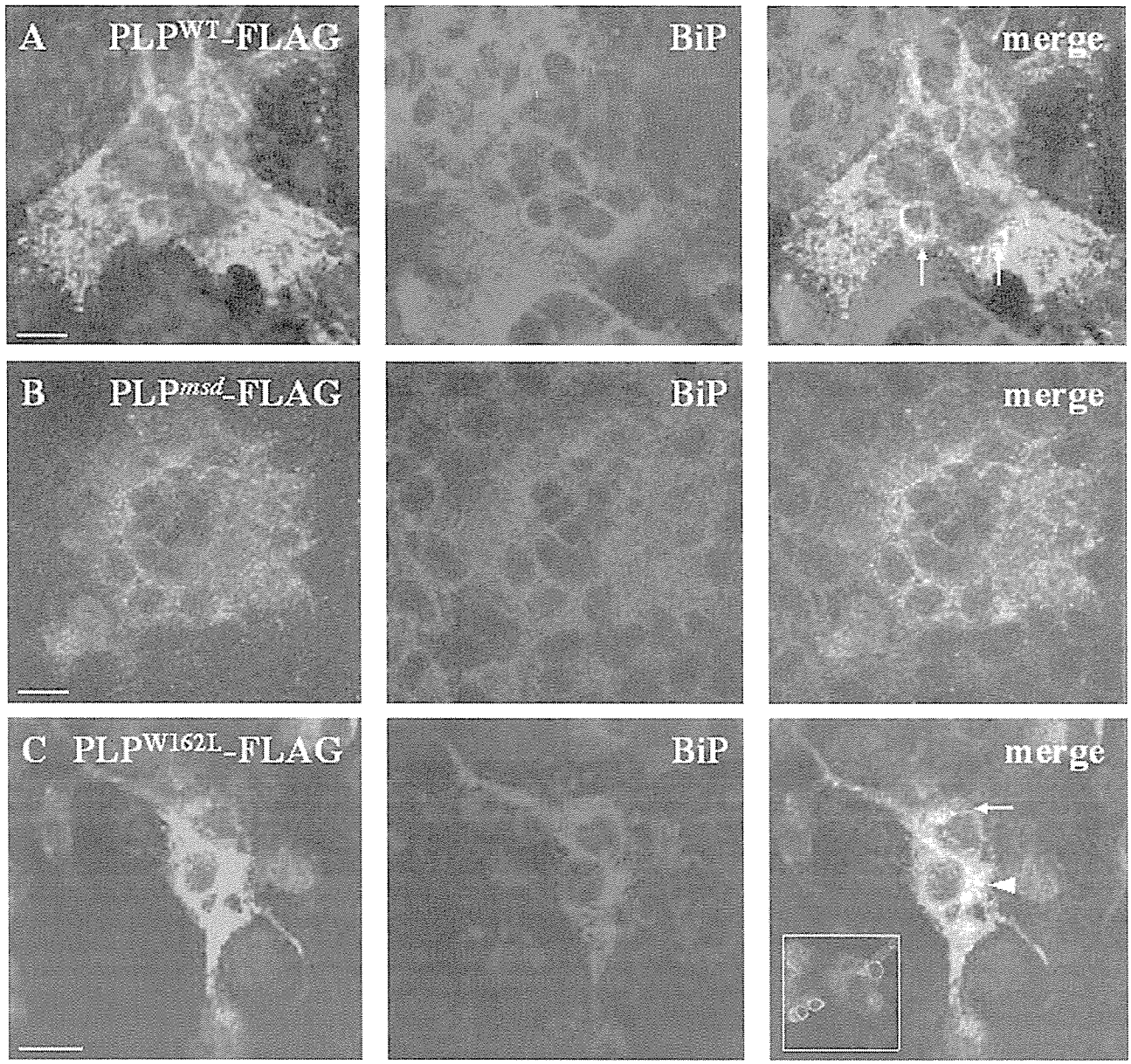

Fig. 6. Transiently transfected PLP-FLAGs in paraformaldehyde-fixed cells detected by immunofluorescence and laser scanning microscopy. COS-7 cells adhering to glass coverslips were transiently transfected with PLP^{WT}-FLAG (A), PLP^{msd}-FLAG (B), or PLP^{W162L}-FLAG (C). After 20 h of transfection, PLP-FLAGs were detected (green) by anti-FLAG immunostaining followed by Alexa 488-conjugated anti-rabbit IgG. ER was simultaneously stained (red) using a combination of anti-KDEL (BiP) antibody and Alexa 546-conjugated anti-mouse IgG. Yellow color is indicative of colocalized PLP-EGFPs and ER. Arrows in A indicate partial ER localization of PLP^{WT}-FLAG. The arrow and arrowhead in C indicate weak and partial colocalization of PLP^{W162L}-FLAG with ER, respectively. The inset in C indicates perinuclear rim localization of PLP^{W162L}-FLAG. Panels are representative, merged, single confocal images of independent triplicate experiments. Scale bars=20 μm.

the ER (Fig. 4D). We observed distinct subcellular localizations for ER and PLP^{W162L}-EGFP within most cells 40 h after transfection (Fig. 4D) and some PLP^{W162L}-EGFP was found in the NE. This is consistent with previous reports showing that accumulation of torsinA mutants at the NE is discernable from diffuse perinuclear localization of the ER (Gonzalez-Alegre and Paulson, 2004; Goodchild and Dauer, 2004). This NE-accumulation may help to explain why PLP^{W162L} does not reach the cell surface even though it passes through the ER. In this case, it is not expected that the UPR is induced. This hypothesis is consistent with the finding that the UPR is not activated by overexpression of a NE-accumulating mutant torsinA that causes DYT1 dystonia (Gonzalez-Alegre and Paulson, 2004). There may be specific quality control mechanisms for mutant proteins accumulating in the NE.

In this report, we provide evidence that a disease-associated PLP^{W162L} is not retained in the ER after translation in COS-7 cells. Absence of mutant PLP in the ER might be associated with the mild clinical symptoms

of PLP^{W162L} as is the case with PMDs associated with a null mutation of the *PLP1* gene (Raskind et al., 1991; Sistermans et al., 1996; Inoue et al., 2002). Our case supports the idea that variable PMD severity caused by missense mutations is consistent with a graded UPR from the ER. Moreover, we showed that PLP^{W162L}-EGFP unexpectedly accumulates in the NE. Aberrant subcellular distribution of mutant PLP in the NE has never been described in either PMD patients or cells transfected with mutant *PLP1* cDNA. Further, *in vivo* analyses are required to elucidate the significance of this in the pathology of PMD.

Acknowledgments—We thank K. Kikuchi for technical assistance and K. Inoue for critical review of the manuscript.

REFERENCES

Boespflug-Tanguy O, Mimault C, Melki J, Cavagna A, Giraud G, Pham Dinh D, Dastugue B, Dautigny A (1994) Genetic homogeneity of Pelizaeus-Merzbacher disease: tight linkage to the proteolipoprotein locus in 16 affected families. PMD Clinical Group. Am J Hum Genet 55:461–467.

Boucher SE, Cypher MA, Carlock LR, Skoff RP (2002) Proteolipid protein gene modulates viability and phenotype of neurons. J Neurosci 22:1772–1783.

Cerghet M, Bessert DA, Nave KA, Skoff RP (2001) Differential expression of apoptotic markers in jimpy and in Plp overexpressors: evidence for different apoptotic pathways. J Neurocytol 30:841–855.

Gentzsch M, Chang XB, Cui L, Wu Y, Ozols VV, Choudhury A, Pagano RE, Riordan JR (2004) Endocytic trafficking routes of wild type and DeltaF508 cystic fibrosis transmembrane conductance regulator. Mol Biol Cell 15:2684–2696.

Ghandour MS, Feutz AC, Jalabi W, Taleb O, Bessert D, Cypher M, Carlock L, Skoff RP (2002) Trafficking of PLP/DM20 and cAMP signaling in immortalized jimpy oligodendrocytes. Glia 40:300–311.

Gonzalez-Alegre P, Paulson HL (2004) Aberrant cellular behavior of mutant torsinA implicates nuclear envelope dysfunction in DYT1 dystonia. J Neurosci 24:2593–2601.

Goodchild RE, Dauer WT (2004) Mislocalization to the nuclear envelope: an effect of the dystonia-causing torsinA mutation. Proc Natl Acad Sci U S A 101:847–852.

Gow A (2003) The COS-7 cell in vitro paradigm to study myelin proteolipid protein 1 gene mutations. Methods Mol Biol 217:263–275.

Gow A, Friedrich VL Jr, Lazzarini RA (1994a) Intracellular transport and sorting of the oligodendrocyte transmembrane proteolipid protein. J Neurosci Res 37:563–573.

Gow A, Friedrich VL Jr, Lazzarini RA (1994b) Many naturally occurring mutations of myelin proteolipid protein impair its intracellular transport. J Neurosci Res 37:574–583.

Gow A, Lazzarini RA (1996) A cellular mechanism governing the severity of Pelizaeus-Merzbacher disease. Nat Genet 13:422–428.

Gow A, Sharma R (2003) The unfolded protein response in protein aggregating diseases. Neuromolecular Med 4:73–94.

Gow A, Southwood CM, Lazzarini RA (1998) Disrupted proteolipid protein trafficking results in oligodendrocyte apoptosis in an animal model of Pelizaeus-Merzbacher disease. J Cell Biol 140:925–934.

Griffiths I, Klugmann M, Anderson T, Thomson C, Vouyiouklis D, Nave KA (1998) Current concepts of PLP and its role in the nervous system. Microsc Res Tech 41:344–358.

Hudson LD, Puckett C, Berndt J, Chan J, Gencic S (1989) Mutation of the proteolipid protein gene PLP in a human X chromosome-linked myelin disorder. Proc Natl Acad Sci U S A 86:8128–8131.

Inoue K (2005) PLP1-related inherited dysmyelinating disorders: Pelizaeus-Merzbacher disease and spastic paraplegia type 2. Neurogenetics 6:1–16.

Inoue K, Osaka H, Thurston VC, Clarke JT, Yoneyama A, Rosenbarker L, Bird TD, Hodes ME, Shaffer LG, Lupski JR (2002) Genomic rearrangements resulting in PLP1 deletion occur by nonhomologous end joining and cause different dysmyelinating phenotypes in males and females. Am J Hum Genet 71:838–853.

Kagawa T, Ikenaka K, Inoue Y, Kuriyama S, Tsujii T, Nakao J, Nakajima K, Aruga J, Okano H, Mikoshiba K (1994) Glial cell degeneration and hypomyelination caused by overexpression of myelin proteolipid protein gene. Neuron 13:427–442.

Kaufman RJ (2002) Orchestrating the unfolded protein response in health and disease. J Clin Invest 110:1389–1398.

Naismith TV, Heuser JE, Breakefield XO, Hanson PI (2004) TorsinA in the nuclear envelope. Proc Natl Acad Sci U S A 101:7612–7617.

Osaka H, Kawanishi C, Inoue K, Onishi H, Kobayashi T, Sugiyama N, Kosaka K, Nezu A, Fujii K, Sugita K, Kodama K, Murayama K, Murayama S, Kanazawa I, Kimura S (1999) Pelizaeus-Merzbacher disease: three novel mutations and implication for locus heterogeneity. Ann Neurol 45:59–64.

Raskind WH, Williams CA, Hudson LD, Bird TD (1991) Complete deletion of the proteolipid protein gene (PLP) in a family with X-linked Pelizaeus-Merzbacher disease. Am J Hum Genet 49: 1355–1360.

Readhead C, Schneider A, Griffiths I, Nave KA (1994) Premature arrest of myelin formation in transgenic mice with increased proteolipid protein gene dosage. Neuron 12:583–595.

Roussel G, Neskovic NM, Trifilieff E, Artault JC, Nussbaum JL (1987) Arrest of proteolipid transport through the Golgi apparatus in Jimpy brain. J Neurocytol 16:195–204.

Schneider A, Montague P, Griffiths I, Fanarraga M, Kennedy P, Brophy P, Nave KA (1992) Uncoupling of hypomyelination and glial cell death by a mutation in the proteolipid protein gene. Nature 358:758–761.

Sharma M, Pampinella F, Nemes C, Benharouga M, So J, Du K, Bache KG, Papsin B, Zerangue N, Stenmark H, Lukacs GL (2004) Misfolding diverts CFTR from recycling to degradation: quality control at early endosomes. J Cell Biol 164:923–933.

Simons M, Kramer EM, Macchi P, Rathke-Hartlieb S, Trotter J, Nave KA, Schulz JB (2002) Overexpression of the myelin proteolipid protein leads to accumulation of cholesterol and proteolipid protein in endosomes/lysosomes: implications for Pelizaeus-Merzbacher disease. J Cell Biol 157:327–336.

Sistermans EA, de Wijs IJ, de Coo RF, Smit LM, Menko FH, van Oost BA (1996) A (G-to-A) mutation in the initiation codon of the proteolipid protein gene causing a relatively mild form of Pelizaeus-Merzbacher disease in a Dutch family. Hum Genet 97:337–339.

Southwood CM, Garbern J, Jiang W, Gow A (2002) The unfolded protein response modulates disease severity in Pelizaeus-Merzbacher disease. Neuron 36:585–596.

Thomson CE, Montague P, Jung M, Nave KA, Griffiths IR (1997) Phenotypic severity of murine Plp mutants reflects in vivo and in vitro variations in transport of PLP isoproteins. Glia 20:322–332.

APPENDIX

Supplementary data

Supplementary data associated with this article can be found, in the online version, at doi: 10.1016/j.neuroscience.2006.05.067.

(Accepted 22 May 2006)
(Available online 14 July 2006)

Spanish Fondo de Investigación Sanitaria (FIS-04-0009, E. L.-G., J. M.), and Networks for Mitochondrial Disorders and Ataxias (G03-011/G03-056, M.P., A.O., E. L.-G., A.N., A.S., M.D. H., M.A.V., P.B., J.M., R.A.).

References

1. Zeviani M, Moraes CT, DiMauro S, et al. Deletions of mitochondrial DNA in Kearns-Sayre syndrome. Neurology 1988;38: 1339–1346.
2. Allen J, DiMauro S, Coulter D, et al. Kearns-Sayre syndrome with reduced plasma and cerebrospinal fluid folate. Ann Neurol 1983;13,6:679–681.
3. Dougados M, Zittoun J, Laplane D, Castaigne P. Folate metabolism disorder in Kearns-Sayre syndrome. Ann Neurol 1983; 13:679–682.
4. Artuch R, Vilaseca MA, Farré C, Ramón F. Determination of lactate, pyruvate, B-hydroxybutyrate and acetoacetate with a centrifugal analyser. Eur J Clin Chem Clin Biochem 1995;33: 529–533.
5. Moyano D, Vilaseca MA, Artuch R, Lambruschini N. Plasma amino acids in anorexia nervosa. Eur J Clin Nutr 1998;52: 684–689.
6. Belz S, Frickel C, Wolfrom C, et al. High-performance liquid chromatographic determination of methotrexate, 7-hydroxymethotrexate, 5-methyltetrahydrofolic acid and folinic acid in serum and cerebrospinal fluid. J Chromatogr B Biomed Appl 1994;661:109–118.
7. Ormazabal A, García-Cazorla A, Fernández Y, et al. HPLC with electrochemical and fluorescence detection procedures for the diagnosis of inborn errors of biogenic amines and pterins. J Neurosci Methods 2005;142:153–158.
8. Rustin P, Chretien D, Bourgeron T, et al. Biochemical and molecular investigations in respiratory chain deficiencies. Clin Chim Acta 1994;228:35–51.
9. Fischer JC, Ruitenbeek W, Berden Já, et al. Differential investigation of the capacity of succinate oxidation in human skeletal muscle. Clin Chim Acta 1985;153:23–36.
10. Lowry OH, Rosenbrough NJ, Farr AL, Randall RJ. Protein measurement with the folin phenol reagent. J Biol Chem 1951; 193:265–275.
11. Barragan-Campos HM, Vallee JN, Lo D, Barrera-Ramirez CF, et al. Brain magnetic resonance imaging findings in patients with mitochondrial cytopathies.Arch Neurol 2005;62:737–742.
12. Ramaekers VT, Blau N. Cerebral folate deficiency. Dev Med Child Neurol 2004;46:843–851.
13. Tanji K, Schon EA, DiMauro S, Bonilla E. Kearns-Sayre syndrome: oncocytic transformation of choroids plexus epithelium. J Neurol Sci 2000;178:29–36.
14. Surtees R, Leonard J, Austin S. Association of demyelination with deficiency of cerebrosinal-fluid S-adenosylmethionine in inborn errors of methyl-transfer pathway. Lancet 1991;338: 1550–1554.
15. Ramaekers VT, Rothenberg SP, Sequeira JM, et al. Autoantibodies to folate receptors in the cerebral folate deficiency syndrome. N Engl J Med 2005;352:1985–1991.
16. Surtees R, Heales S, Bowron A. Association of cerebrospinal fluid deficiency of 5-methyltetrahydrofolate, but not S-adenosylmethionine, with reduced concentrations of the acid metabolites of 5-hydroxytryptamine and dopamine. Clin Sci 1994;86:697–702.
17. Hansen FJ, Blau N. Cerebral folate deficiency: life-changing supplementation with folinic acid. Mol Genet Metab 2005;84: 371–373.
18. Crott JW, Choi SW, Branda RF, Mason JB. Accumulation of mitochondrial DNA deletions is age, tissue and folate-dependent in rats. Mut Res 2005;570:63–70.

Spastic Paraplegia Type 2 Associated with Axonal Neuropathy and Apparent *PLP1* Position Effect

Jennifer A. Lee, BS,[1] Ricardo E. Madrid, MD,[2] Karen Sperle, MS,[3] Carolyn M. Ritterson, BS,[4] Grace M. Hobson, PhD,[3,5] James Garbern, MD, PhD,[6] James R. Lupski, MD, PhD,[1,7,8] and Ken Inoue, MD, PhD[1,9]

Objective: **To report an association between spastic paraplegia type 2 with axonal peripheral neuropathy and apparent proteolipid protein gene (*PLP1*) silencing in a family.** ***Methods:*** **Pulsed-field gel electrophoresis, custom array comparative genomic hybridization, and semi-quantitative multiplex polymerase chain reaction analyses were used to examine the *PLP1* genomic region.** ***Results:*** **Electrodiagnostic studies and a sural nerve biopsy showed features of a dystrophic axonal neuropathy. Molecular studies identified a small duplication downstream of *PLP1*.** ***Interpretation:*** **We propose the duplication to result in *PLP1* gene silencing by virtue of a position effect. Our observations suggest that genomic rearrangements that do not include *PLP1* coding sequences should be considered as yet another potential mutational mechanism underlying *PLP1*-related dysmyelinating disorders.**

Ann Neurol 2006;59:398–403

Pelizaeus–Merzbacher disease (PMD) and spastic paraplegia type 2 (SPG2) are clinically distinct allelic disorders, yet represent a wide spectrum of central ner-

From the [1]Department of Molecular and Human Genetics, Baylor College of Medicine, Houston, TX; [2]New York State Institute for Basic Research in Developmental Disabilities, George A. Jervis Clinic, Staten Island, NY; [3]Nemours Biomedical Research, Alfred I. duPont Hospital for Children, Nemours Children's Clinic, Wilmington, DE; [4]Department of Biology, Boston University, Boston, MA; [5]Department of Pediatrics, Jefferson Medical College, Philadelphia, PA; [6]Department of Neurology and Center of Molecular Medicine and Genetics, Wayne State University School of Medicine, Detroit, MI; [7]Department of Pediatrics, Baylor College of Medicine and [8]Texas Children's Hospital, Houston, TX; and [9]Department of Mental Retardation and Birth Defect Research, National Institute of Neuroscience, National Center of Neurology and Psychiatry, Tokyo, Japan.

Received Mar 23, 2005, and in revised form Aug 24 and Sep 28. Accepted for publication Sep 29, 2005.

Published online Dec 22, 2005, in Wiley InterScience (www.interscience.wiley.com). DOI: 10.1002/ana.20732

Address correspondence to Dr Inoue, Department of Mental Retardation and Birth Defect Research National, Institute of Neurology National Center of Neurology and Psychiatry (NCNP), 4-1-1 Ogawahigashi, Kodaira, Tokyo 187-8502.
E-mail: kinoue@ncnp.go.jp

